Accepted Manuscript

Synthesis of a Fluorescent BODIPY-tagged ROMP catalyst and Initial Polymerization-Propelled Diffusion Studies

Jazmin Godoy, Víctor García-López, Lin-Yung Wang, Simon Rondeau-Gagné, Stephan Link, Angel A. Martí, James M. Tour

PII: S0040-4020(15)00517-7

DOI: 10.1016/j.tet.2015.04.027

Reference: TET 26630

To appear in: *Tetrahedron*

Received Date: 27 January 2015

Revised Date: 9 April 2015

Accepted Date: 10 April 2015

Please cite this article as: Godoy J, García-López V, Wang L-Y, Rondeau-Gagné S, Link S, Martí AA, Tour JM, Synthesis of a Fluorescent BODIPY-tagged ROMP catalyst and Initial Polymerization-Propelled Diffusion Studies, *Tetrahedron* (2015), doi: 10.1016/j.tet.2015.04.027.

Synthesis of a Fluorescent BODIPY-tagged ROMP catalyst and Initial Polymerization-Propelled Diffusion Studies

Jazmin Godoy,[1] Víctor García-López,[1] Lin-Yung Wang,[1] Simon Rondeau-Gagné,[1,2] Stephan Link,[1,3] Angel A. Martí,[1,3,4]* and James M. Tour[1,3,4]*

[1]*Department of Chemistry, Rice University, 6100 Main Street, Houston, Texas 77005*

[3]*Smalley Institute for Nanoscale Science and Technology, Rice University, 6100 Main Street, Houston, Texas 77005*

[4]*Department of Materials Science and NanoEngineering, Rice University, 6100 Main Street, Houston, Texas 77005*

[2]*Université Laval, Département de Chimie, Pavillon Alexandre-Vachon Bureau 1407, Laval, Canada 4137*

KEYWORDS

nanomachines, fluorescence correlation spectroscopy, fluorescent Hoveyda-Grubbs catalyst, BODIPY, ring-opening metathesis polymerization, diffusion coefficient

Corresponding author

* (A. M.) E-mail: amarti@rice.edu

*(J.M.T) E-mail: tour@rice.edu

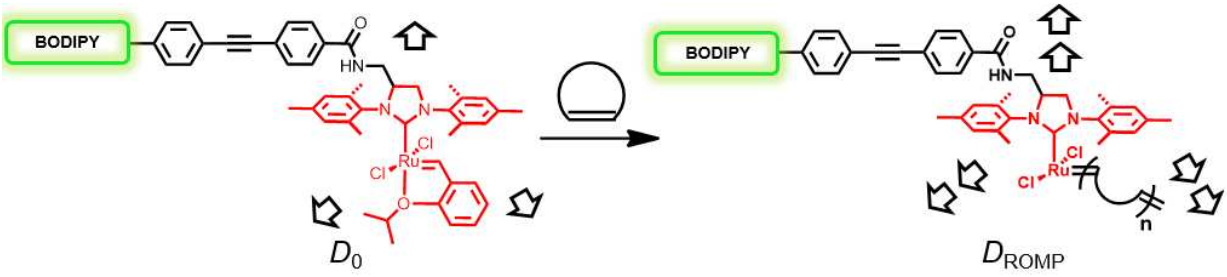

ABSTRACT

The synthesis of a Ru-based olefin metathesis catalyst dye-tagged at the *N*-heterocyclic carbene ligand is reported. Its catalytic activity toward ring-opening metathesis polymerization (ROMP) of 1,5-cyclooctadiene was found to be similar to that of its parent second-generation Hoveyda-Grubbs catalyst. The quantum yield of fluorescence (Φ_F = 0.22) makes it a good candidate to explore, by fluorescence correlation spectroscopy, the potential of a ROMP process to provide a molecule with sufficient energy for self-propulsion in solution.

1. Introduction

Biological machines that convert chemical energy to mechanical work, such as RNA polymerase,[1] ATP synthase,[2] and linear kinesin,[3] inspired scientists to develop artificial nanomachines[4] and nanovehicles.[5]

A family of nanovehicles, termed nanocars,[6] has been synthesized and designed by our group with the goal to roll on surfaces and do work at the nanoscale. One of the challenges to achieving work is the conversion of energy inputs into controlled molecule transportation. In 2006, our group reported a light-driven motorized nanocar.[7] The design included a unidirectional rotatory motor, capable of rotating at 1.8 rotations per h at 60 °C, with an oligo(phenylene ethylene) chassis and axle system and four carboranes that served as the wheels. Later we reported the synthesis of a nanocar with ~3 MHz rotation speed.[8] The

synthesis of a chemically propelled nanocar has also been reported.[9] The propulsion was generated by a ring-opening metathesis polymerization (ROMP) that was achieved by incorporation of a Hoveyda-Grubbs catalyst.

Concomitantly, a number of chemically propelled micro-motors have been developed to operate in solution. Interesting examples of these include bimetallic nanorods that use the catalytic dismutation of H_2O_2 to induce translational movement,[10] and silica particles equipped with a H_2O_2 disproportionation catalyst.[11] However, these systems range from hundreds of nanometers to micrometers in size and small by-product molecules are produced during the propulsion.

An attractive alternative is to explore, in synthetic systems, the potential of a polymerization process to propel motion at the nanoscale, given that this mechanism of propulsion is already present in nature. For example, the movement of the bacterium *listeria monocytogenes* is driven by the polymerization of actin.[12]

Indeed, it was demonstrated that gold-silica Janus particles functionalized with a ROMP catalyst can be propelled by a polymerization process.[13] Upon addition of the cyclic olefin norbornene, the diffusion constant increased up to 70%. These particles, however, are approximately 500 nm in diameter.

Although there are many examples of synthetic rotatory and chemically propelled motors, their potential to promote solution-phase locomotion at the molecular level remains unexplored.'[10,11,13,14] Sen and coworkers observed by NMR spectroscopy that the diffusion coefficient of second generation Grubbs catalyst increased up to 50% during ring closing metathesis (RCM).[15]

The objective of the present work is to investigate the potential of a ROMP process to provide locomotion at the molecular level. One method to monitor the diffusion of molecules in solution is fluorescence correlation spectroscopy (FCS).[16] Therefore, to test our hypothesis using FCS to monitor movement, it was necessary to synthesize a fluorescent ROMP catalyst.

2. Results and discussion

2.1 Synthesis of BODIPY-tagged ROMP catalysts

A number of different types of ROMP catalysts have been developed; the Ru-based Hoveyda-Grubbs type (Figure 1) was selected for this study due to its high catalytic activity and relatively higher stability toward air and moisture when compared to other types of catalyst.[17] There are three main approaches commonly used to functionalize a Hoveyda-Grubbs catalyst.[18] Of those, functionalization at the *N*-heterocyclic carbene (NHC) ligand is the most widely used, because the NHC is not exchanged during the ROMP process, thereby providing permanent tagging. For this reason we focused on the preparation of Hoveyda-Grubbs ROMP catalysts dye-tagged at the NHC ligand.

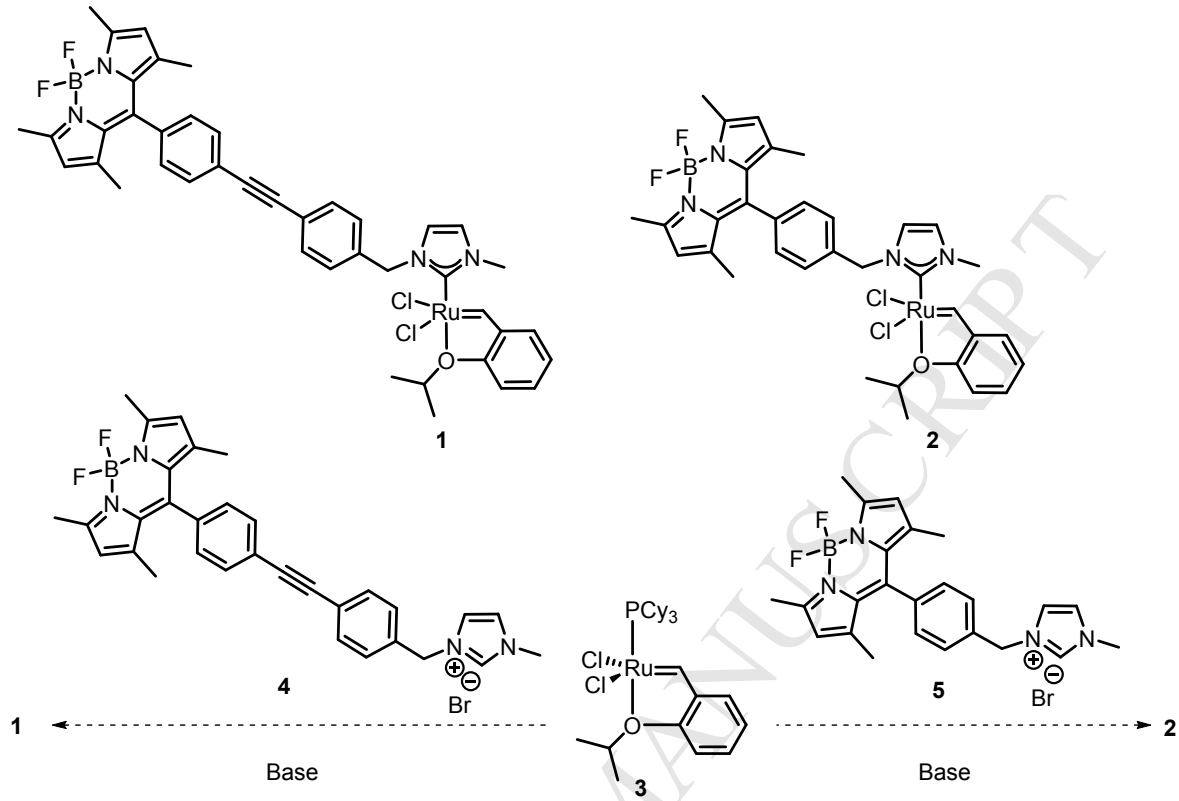

Figure 1. Desired structures of the fluorescent Hoveyda-Grubbs catalysts **1** and **2** and the final step of the proposed syntheses.

The initial targets of fluorescently labeled ROMP catalysts are presented in Figure 1. They feature a 4,4-difluoro-4-bora-3a,4a-diaza-*s*-indacene (BODIPY)[19] dye attached to the ruthenium complex through the NHC ligand. It was envisioned that catalysts **1** and **2** could be prepared through a ligand exchange reaction between the 1st generation Hoveyda-Grubbs catalyst (**3**)[20] and the corresponding carbenes of imidazolium salts **4** and **5**, respectively. The difference between **1** and **2** is the distance between the BODIPY core and the catalytic center. The ethynylene-phenylene spacer of **1** was included to evaluate the effect of the spacer on the formation of the NHC carbene.

The synthesis of BODIPY imidazolium salt **4** started with a Sonogashira coupling between iodophenylene BODIPY **6**[21] and 4-ethynylbenzyl alcohol[22] (Scheme 1). The resultant benzylic alcohol **7** reacted with PBr_3 in presence of catalytic DMF to replace the hydroxyl group with a bromide. Finally, alkylation of the benzylic bromide **8** with 1-methylimidazole afforded **4** in excellent yield.

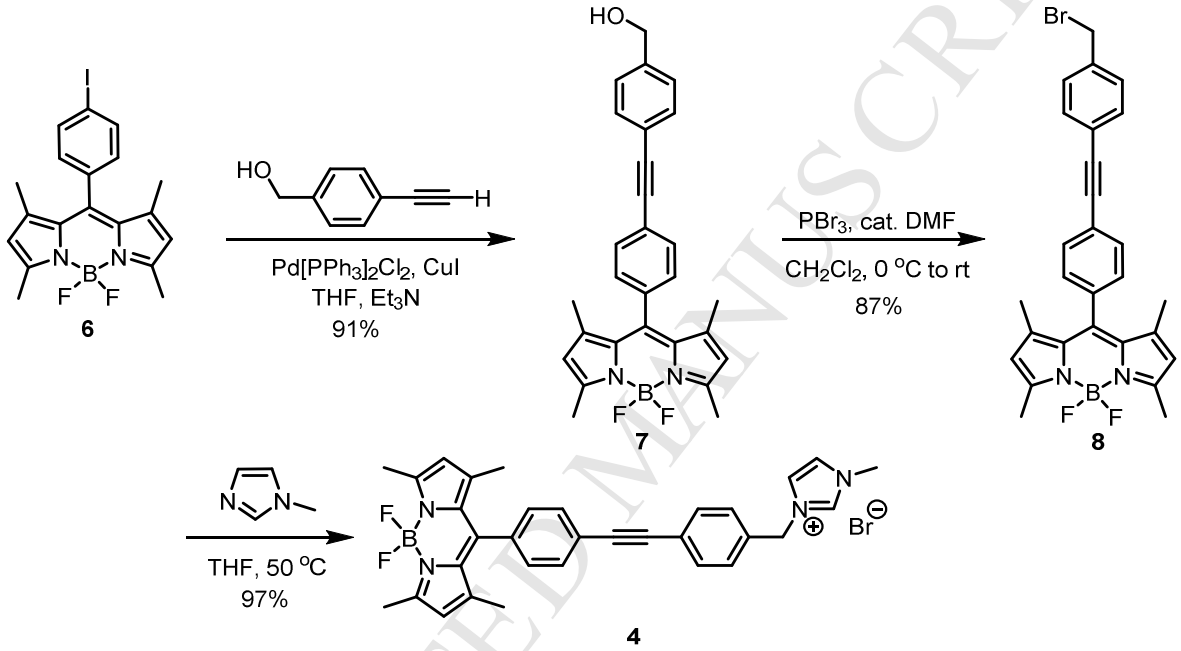

Scheme 1. Synthesis of BODIPY imidazolium salt **4**.

The synthesis of **5** followed a similar approach (Scheme 2). Hydroxymethylphenylene BODIPY **9**[23] was treated with PBr_3 to give the benzylic bromide **10**. The imidazolium salt **5** was obtained in high yield by alkylation of **10** with 1-methylimidazole. With imidazolium salts **4** and **5** in hand, the formation of the corresponding carbenes and subsequent ligand exchange with **3** was investigated. Although many of the common methods to generate NHC carbenes[24] were tried, in all the experiments the imidazolium salts decomposed and no desired product was detected (Figure S1). While the cause for the decomposition of the BODIPY imidazolium salt

was unclear, it was observed that the decomposition occurred during preparation of the NHC carbene. Perhaps the decomposition was due to instability of the carbenes facilitated by the low steric shielding provided by the alkyl imidazole substituents. The reported examples of 1,3-dialkyl-imidazolin-2-ylidene-containing metathesis catalysts have involved the use of bulky alkyl substituents, including cyclohexyl and *tert*-butyl groups.[25]

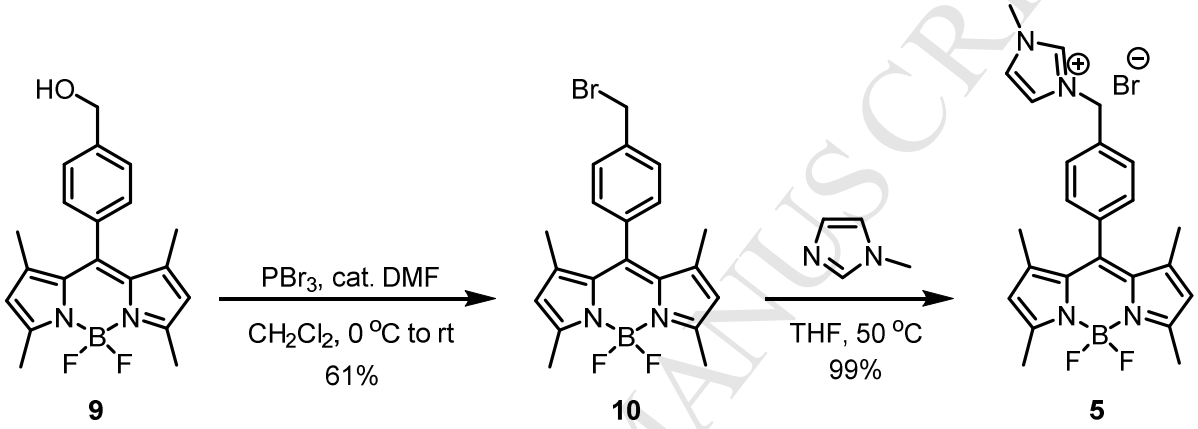

Scheme 2. Synthesis of BODIPY imidazolium salt **5**.

Hence, a new strategy was devised in which no NHC carbene would be generated in presence of BODIPY. The new target, **11** was synthesized in four straightforward steps from previously reported compounds (Scheme 3). Iodo-BODIPY **6** was coupled with 4-ethynylbenzoic acid[26] under conventional Sonogashira coupling conditions. The crude BODIPY carboxylic acid was esterified with pentafluorophenol in the presence of *N*,*N*'-dicyclohexylcarbodiimide (DCC) to give BODIPY pentafluorophenol ester **12**. Separately, Boc-protected Hoveyda-Grubbs complex **13**[27] was deprotected with hydrogen chloride. Finally, BODIPY ester **12** was coupled with the catalyst terminal amine to give **11** through formation of an amide bond.

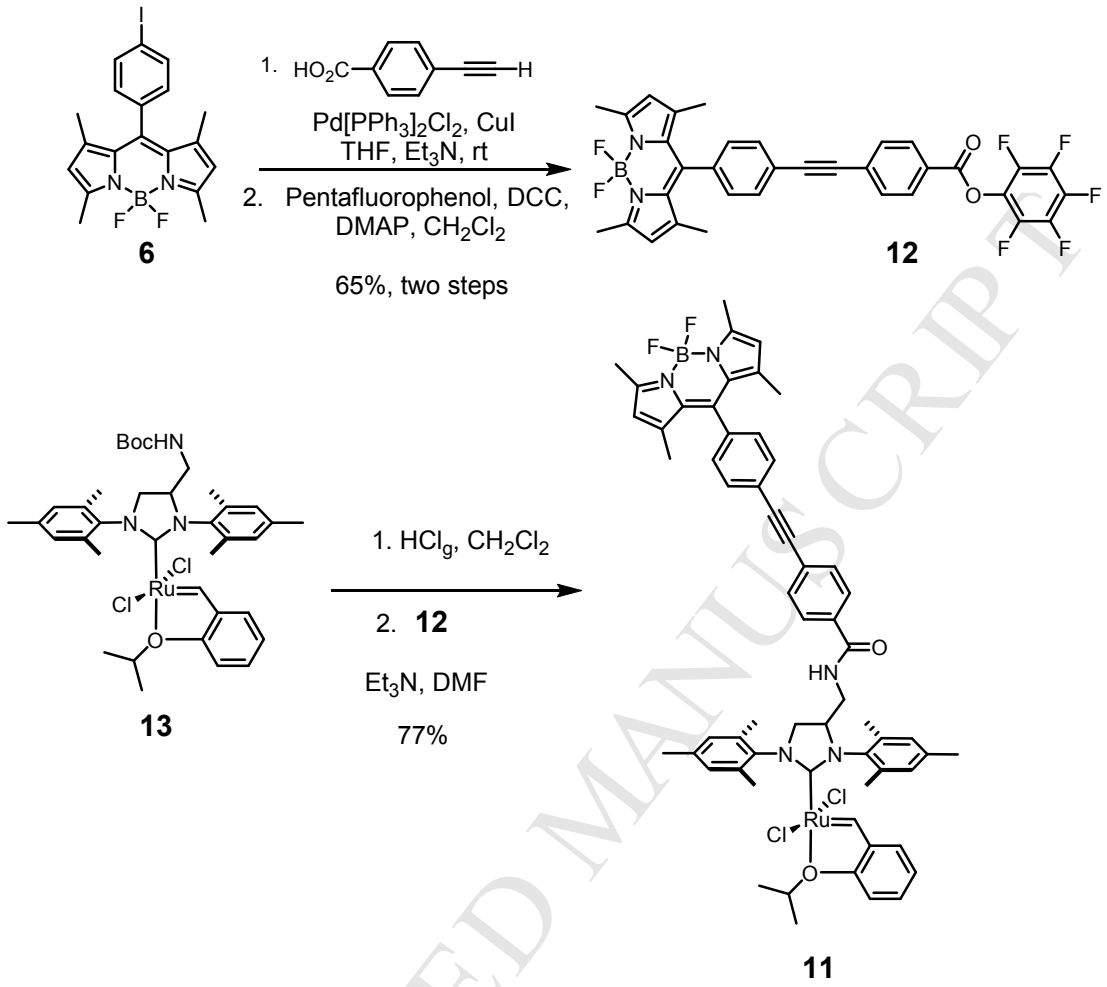

Scheme 3. Synthesis of BODIPY Hoveyda-Grubbs catalyst **11.**

2.3 Fluorescence characterization

Since our current FCS setup requires excitation of the molecules with a 514 or 532 nm laser, it is a prerequisite that the BODIPY catalyst **11** exhibit adequate absorption at either of those wavelengths. As depicted in Figure 2A, **11** absorbs strongly in this region, with its λ_{max} = 504 nm (ε = 72 000 $M^{-1}cm^{-1}$, CH_2Cl_2).

A second requirement is an acceptable fluorescence quantum yield (Φ_F). In dichloromethane, catalyst **11** has Φ_F = 0.22. This value is significantly smaller than the fluorescence quantum yield of its precursor BODIPY **6** (Φ_F = 0.46, CH_2Cl_2).[28] Nonetheless, Φ_F = 0.22 is sufficient for FCS studies.

We reason that the decrease in the fluorescence of **11** could be attributed to the Ru center, given that some Ru-based metathesis catalysts exhibit absorption bands that span across the 500 nm region and lead to through-space fluorescence quenching of neighboring fluorophores *via* fluorescence resonance energy transfer (FRET).[29] However, 2nd generation Hoveyda-Grubbs catalyst (**14**)[30] showed a blueshift in the absorption spectrum at 300-450 nm (Figure 2B), indicating that an intramolecular FRET process is not favorable in our system.

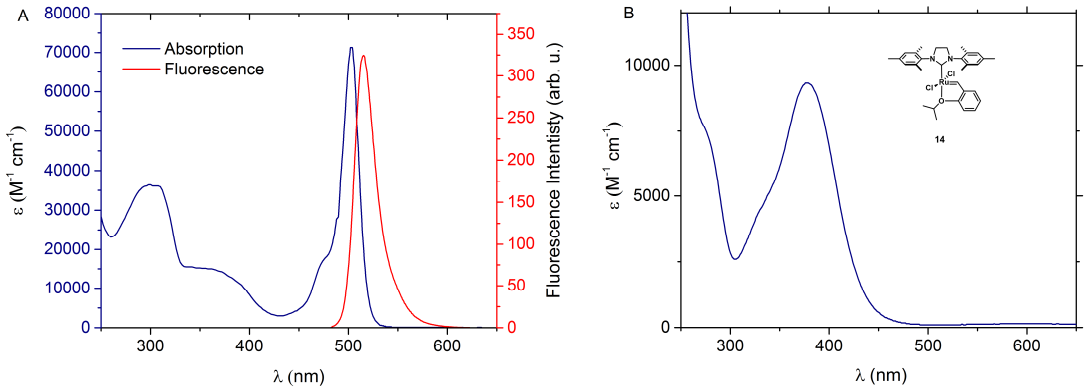

Figure 2. Absorption and fluorescence spectra of **11** and absorption spectrum of **14**. A) UV-vis absorption (blue line) and fluorescence (red line) spectra of **11** in CH_2Cl_2. Excitation at 488 nm B) UV-vis absorption spectrum of the 2nd generation Hoveyda-Grubbs catalyst (**14**) in CH_2Cl_2.

To investigate the potential of intermolecular energy transfer, we measured the lifetimes (τ) of catalyst **11,** BODIPY **12** and BODIPY **6** by using time correlated single photon counting. Figure 3 shows a monoexponential fluorescence decay for BODIPY **6** (τ = 2.99 ns), and

BODIPY **12** (τ = 1.87 ns), whereas **11** has a biexponential decay with shorter lifetimes, τ_1 = 0.63 ns and τ_2 = 1.64 ns. Although the lifetimes of **11** were shorter, the addition of 5 equivalents of 2nd generation Hoveyda-Grubbs catalyst **14** to either catalyst **11** or BODIPY **6** did not generate substantial changes in their lifetimes (Figure S2), demonstrating the absence of intermolecular FRET. Therefore, the drop in the fluorescence yield of **11** compared to **6** is probably due to the extended conjugation introduced by the ethynylene-phenylene functionality in **11**. The decrease in lifetime of **11** compared to **12** is due to the covalent attachment of the Grubbs catalyst.

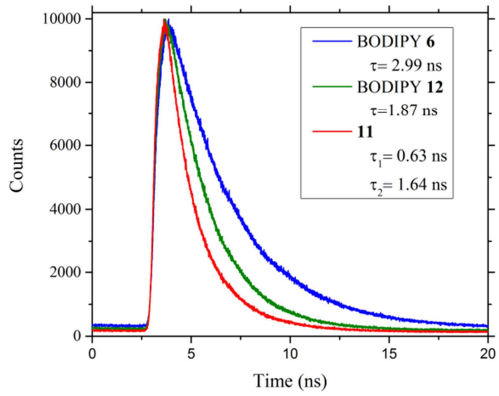

Figure 3. Time-resolved fluorescence decay of BODIPY **6**, **11** and **12** in CH_2Cl_2.

Table 1. Fluorescence properties of BODIPY derivatives.

	λ_{abs} (nm)	λ_{em} (nm)	Φ_F	τ (ns)
BODIPY **6**	504	514	0.46	2.99
BODIPY **12**	504	514	0.27	1.87
11	505	515	0.22	0.63, 1.64

2.4 Catalytic activity of BODIPY-tagged ROMP catalyst

The catalytic activity of **11** toward ROMP of *cis*,*cis*,-1,5-cyclooctadiene (cod) was evaluated in accordance with the standard protocol developed by Grubbs,[31] by collecting a series of ^{1}H NMR spectra to determine the degree of polymerization. One of the reasons for choosing

cod was its relatively slow polymerization rate when compared to more highly strained cyclic olefins such as norbornene. Indeed, 97% of the cod had reacted by the time the first spectrum was collected at 4.2 min (Figure 4). The high activity of **11** was similar to its parent second generation Hoveyda-Grubbs catalyst **14** (Table S1), which afforded 99% conversion of cod at 4.1 min.[31]

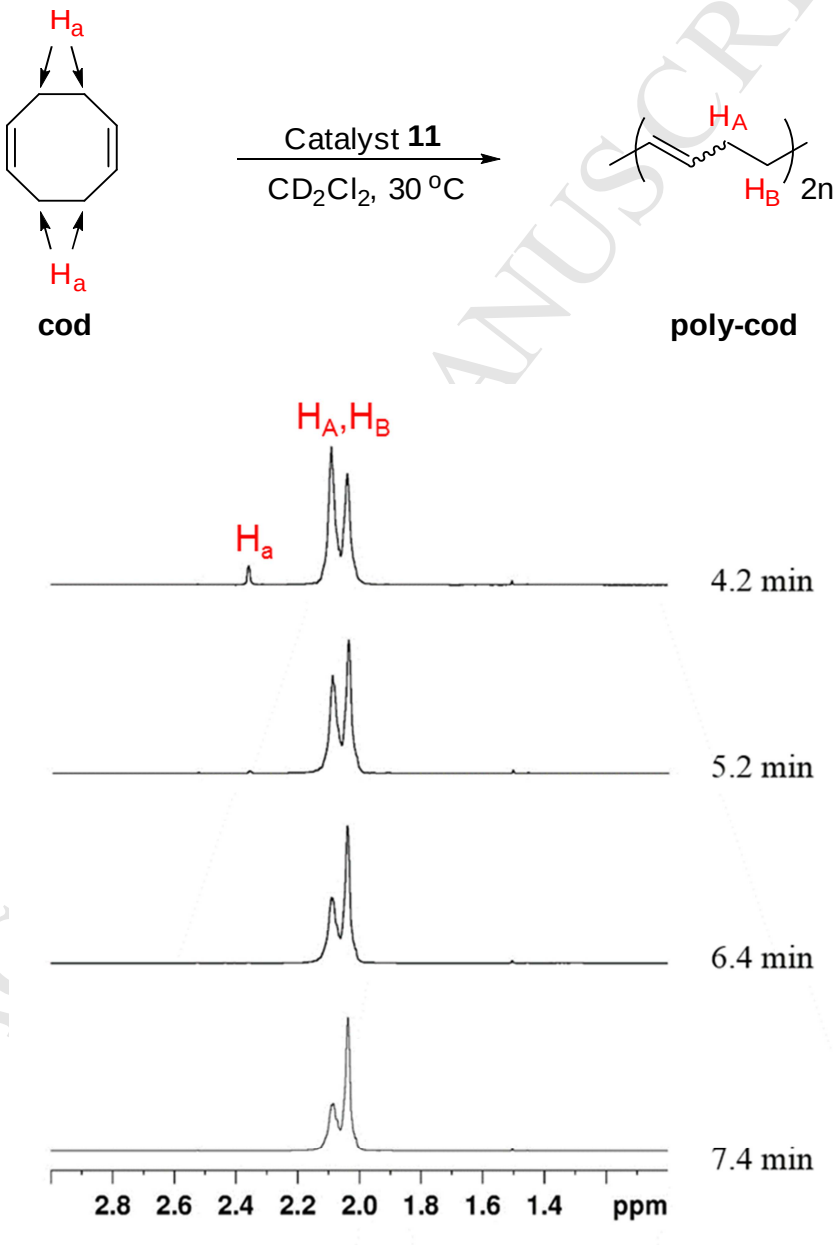

Figure 4. ^{1}H-NMR kinetics of ring-opening metathesis polymerization of cod catalyzed by **11**. After 4.2 min 97% of the cod had reacted. 470 mM of cod, 0.1 mmol % of **11** (0.470 mM), 30 °C, CD_2Cl_2.

2.5 Preliminary diffusion studies

In addition to being a highly active catalyst, **11** is stable under inert conditions. The catalytic activity of a sample stored inside a glove box over two months remained nearly unchanged. The high catalytic activity along with the above discussed optical properties made **11** an excellent candidate to study the potential of a polymerization process to induce motion at the molecular level, using FCS.

The diffusion of catalyst **11** was monitored through FCS, using a custom-built setup (see Supporting Information). For comparison, the diffusion of BODIPY **6** was also measured. Then the diffusion coefficients of catalyst **11** and BODIPY **6** were determined in the presence of either cod or norbornene. Although we expected faster diffusion in the presence of cod, the diffusion coefficient of **11** instead decreased because of the formation of polymer chains as was evident from a film that formed in the sample holder during the FCS measurements (Figure S3). We therefore attribute the smaller diffusion coefficient of **11** in the presence of cod to an increase in the viscosity of the solution. To account for this potential change in viscosity of the medium, we measured the changes in the diffusion of **6** before and after addition of cod to a mixture of **6** and catalyst **14**. The diffusion of **6** decreased upon addition of cod. A correction factor was defined as the ratio of the diffusion coefficients of BODIPY **6** after and before adding cod. In this process, the change in diffusion coefficient is entirely due to the change in viscosity as a result of the polymerization. This factor was then used to correct the diffusion coefficient of **11** in the presence of cod. (Figure S4).

After correcting for the viscosity change, the result showed an increase in the average diffusion coefficients (Figure S4). However, the large standard deviation of the experimental data prevents us from rendering a more confident conclusion, although multiple conditions were explored. Therefore, it is likely that the heterogeneity of the system was the cause of the large variability in the results.

3. Conclusion

In summary we synthesized a permanent fluorescent Hoveyda-Grubbs ROMP catalyst dye-tagged at the NHC ligand. The catalytic activity of this complex toward ROMP was found to be similar to that of its non-fluorescent analogue. We were able to study its diffusion via FCS although no substantial increase was observed due to the hetereogenity of the system caused by the precipitation of the polymer.

4. Experimental section

4.1 ROMP of 1,5-Cyclooctadiene.[31]

Dichloromethane-d2 was freeze/pump/thawed 3×. *cis*,*cis*,-1,5-Cyclooctadiene (cod) was distilled over CaH_2 immediately prior to the polymerization reaction. As reported by Grubbs,[31] we also found that aged cod gave considerably lower rates. ^{1}H NMR spectra were collected at 500 MHz. Inside a glove box, an NMR tube with a septum/screw-cap (model 27093, Sigma-Aldrich) was charged with catalyst solution (0.40 μmol) and CD_2Cl_2 to give a total volume of 0.80 mL. The solution was equilibrated at 30 °C in the NMR probe. The sample was then ejected from the NMR instrument to add cod (50 μL, 0.40 mmol) *via* a syringe. A series of spectra were collected over an appropriate period of time. The degree of conversion to polymer was determined by comparing the ratio of the integrals of the methylene protons in the starting material at δ 2.36 (m) with those in the product at δ 2.09 br (m), δ 2.04 (br m).

4.2 Spectroscopic Measurements.

Absorption spectra were recorded on a Shimadzu UV-3101PC spectrophotometer with a 2 nm slit. The fluorescence spectra were obtained on a Perkin Elmer LS50B instrument, using dichloromethane solutions exposed to air with absorbance between 0.01 − 0.06. Two emission spectra were recorded for each compound and the two quantum yields obtained were then averaged. All fluorescence spectra were corrected. Excitation was done at the corresponding λ_{max} − 30 nm wavelength. Rhodamine 6G was used as the reference (ϕ_{ref} = 0.95 in EtOH, λ_{exc} = 488 nm). The fluorescence quantum yield of **11** was calculated from eq. 1. *F* denotes the integral of the corrected fluorescence spectrum, *A* is the absorbance at the excitation wavelength and *n* is the refractive index of the medium as in eq 1:

$$\Phi_{\mathrm{exp}} = \Phi_{\mathrm{ref}} \frac{F\{1-\exp(-A_{\mathrm{ref}}\ln 10)\}n^2}{F_{\mathrm{ref}}\{1-\exp(-A\ln 10)\}{n_{\mathrm{ref}}}^2} \quad (1)$$

4.3 Time Correlated Single Photon Counting Measurements.

Dichloromethane was distilled over CaH_2 and freeze/pump/thawed 3× immediately prior to the measurements. Six solutions were prepared in a dry box with the following concentrations: **11** (1×10^{-5} M), BODIPY **12** (1×10^{-5} M), BODIPY **6** (1×10^{-5} M), a 1:5 molar mixture of **11** and **14** (1×10^{-5} M), a 1:5 molar mixture of BODIPY **12** and **14** (1×10^{-5} M), and a 1:5 molar mixture of BODIPY **6** and **14** (1×10^{-5} M). Time resolved decays of these solutions were obtained using an Edinburgh Instruments OD470 single-photon counting spectrometer with 443.6 nm ps pulse diode lasers, at 20 ns repetition pulse, 470 nm filter and the detection wavelength was 515 nm. Lifetimes were determined by iterative reconvolution of the decay transients with the Instrument Response Function (IRF) by non-linear least square analysis.

4.4 General synthetic procedures

^{1}H NMR and ^{13}C NMR spectra were recorded at 400 or 500 and 100 or 125 MHz, respectively. Proton chemical shifts (δ) are reported in ppm downfield from tetramethylsilane (TMS). MALDI-TOF of **12** was performed using 2-[(2*E*)-3-(4-*tert*-butylphenyl)-2-methylprop-2-enylidene]malononitrile (DCTB) as the matrix. FTIR spectra were recorded by deposition of the sample on a KBr plate from a CH_2Cl_2 solution using a Nicolet FTIR Infrared Microscope with ATR objective with 2 cm^{-1} slit. All reactions were performed under an atmosphere of nitrogen unless stated otherwise. Reagent grade tetrahydrofuran (THF) and diethyl ether (Et_2O) were distilled from sodium benzophenone ketyl. Triethylamine (TEA) and CH_2Cl_2 were distilled over CaH_2. 2,4-Dimethylpyrrole was distilled from CaH_2 under a nitrogen atmosphere. *cis*,*cis*-1,5-Cyclooctadiene was distilled from CaH_2 under a nitrogen atmosphere. All other chemicals were purchased from commercial suppliers and used without further purification. Flash column chromatography was performed using 230−400 mesh silica gel from EM Science, except for catalyst **12**, which was purified using 40-63 µm Geduran silica gel 60 from EMD Chemicals. Thin layer chromatography was performed using glass plates pre-coated with silica gel 40 F_{254} purchased from EM Science. The syntheses of compounds **6**,[21] 4-ethynylbenzyl alcohol,[22] 4-ethynylbenzoic acid,[26] **9**,[23] and **14**,[30] were performed according to formerly reported protocols.

4.4.1. General Procedure for the Coupling of a Terminal Alkyne with an Aryl Halide Using a Palladium-Catalyzed Cross-Coupling (Sonogashira) Protocol.

To an oven-dried round-bottom flask or screw cap tube equipped with a magnetic stir bar were added the aryl halide, the terminal alkyne, $PdCl_2(PPh_3)_2$ or $PdCl_2(PhCN)_2$ (~ 2 mol % per aryl halide), CuI (~ 4 mol % per aryl halide), and in the case of using $PdCl_2(PhCN)_2$, also ~ 4 mol % per aryl halide of HP(*tert*-Bu)$_3$. A solvent system of TEA and/or THF was added depending on the substrates. Upon completion, the reaction was quenched with a saturated

solution of NH_4Cl. The organic layer was then diluted with diethyl ether or CH_2Cl_2, and washed with water or saturated NH_4Cl (1 ×). The combined aqueous layers were extracted with hexanes, diethyl ether, or CH_2Cl_2 (2 ×). The combined organic layers were dried over $MgSO_4$ and filtered, and the solvent was removed from the filtrate *in vacuo* to afford the crude product, which was purified by column chromatography (silica gel). Eluents and other slight modifications are described below for each compound.

4.4.2. General Procedure for Deprotection of TIPS-Protected Alkynes using TBAF.

In a round-bottomed flask equipped with a magnetic stir bar, the protected alkyne was dissolved in THF ([protected alkyne] = 0.05 − 0.1 M). TBAF in THF (1.0 M, 1.1 equiv per alkyne) was added. The mixture was stirred at rt for 0.5 h or until the reaction was complete (monitored by TLC). The reaction was quenched with a saturated solution of NH_4Cl. The organic layer was then diluted with ethyl acetate. The organic layer was dried over $MgSO_4$ and filtered, and the solvent was removed from the filtrate *in vacuo* to afford the crude product, which was purified by column chromatography (silica gel).

4.5 Synthesis of BODIPY imidazolium salt 4.

4.5.1 4-Ethynylbenzyl alcohol.[24]

See the general procedure for the Pd/Cu coupling reaction. A screw cap tube was used. The materials used were 4-bromobenzyl alcohol (0.280 g, 1.50 mmol), TIPSA (0.50 mL, 2.25 mmol), $PdCl_2(PhCN)_2$ (57.5 mg, 0.15 mmol), CuI (28.0 mg, 0.15 mmol), HP(*tert*-Bu)$_3$ (87.0 mg, 0.30 mmol), TEA (10.0 mL), and THF (10.0 mL) at 70 °C overnight. The residue was purified by flash column chromatography in silica gel using 20% ethyl acetate in hexanes; the product-containing fractions were combined, concentrated and the residue was subjected to the general procedure for the deprotection of TIPS-protected alkynes. The materials used were the TIPS

protected intermediate (349 mg, 1.2 mmol), and TBAF (1.8 mL, 1.0 M in THF). The mixture was stirred at rt for 3 h. The crude terminal alkyne was purified in a silica gel column using 30% ethyl acetate in hexanes as eluent to yield 4-ethynylbenzyl alcohol (131 mg, 0.99 mmol, 67%, two steps) as a brown oil. ^{1}H NMR (400 MHz, $CDCl_3$) δ 7.49 (d, *J* = 8.0 Hz, 2H), 7.32 (d, *J* = 8.0 Hz, 2H), 4.70 (s, 2H), 3.07 (s, 1H).

*4.5.2. BODIPY (**7**).*

See the general procedure for the Pd/Cu coupling reaction. The materials used were BODIPY **6**[21] (610 mg, 1.35 mmol), 4-ethynylbenzyl alcohol[22] (269 mg, 2.03 mmol), $PdCl_2(PPh_3)_2$ (47.4 mg, 0.07 mmol), CuI (26.0 mg, 0.135 mmol), TEA (20.0 mL), and THF (60.0 mL) at rt overnight. The residue was suspended in 35 mL of MeOH. The suspension was heated using an oil bath until the mixture started boiling. The heating was then turned off, and the mixture was allowed to cool inside the oil bath. The resultant solid was filtered under vacuum and washed with cold EtOH. After drying the product in vacuum, BODIPY **7** was obtained as an orange solid (556 mg, 1.22 mmol, 91%). FTIR (neat) 3558, 3116, 3066, 3039, 2954, 2919, 2874.5, 2842, 2786, 2730, 2680, 2347, 2223, 1926, 1619, 1540, 1501.5, 1466, 1401, 1366, 1298,1266, 1183, 1157, 1086, 1039, 968, 824, 765, 703 cm^{-1}; ^{1}H NMR (400 MHz, $CDCl_3$) δ 7.67 (d, *J* = 8.4 Hz, 2H), 7.56 (d, *J* = 8.0 Hz, 2H), 7.38 (d, *J* = 8.0 Hz, 2H), 7.29 (d, *J* = 8.0 Hz, 2H), 5.99 (s, 2H), 4.74 (d, *J* = 5.6 Hz, 2H), 2.56 (s, 6H), 1.43 (s, 6H); ^{13}C NMR (100 MHz, $CDCl_3$) δ 156.0, 143.2, 141.6, 141.0, 135.2, 132.5, 132.0, 131.4, 128.4, 127.1, 124.3, 122.2, 121.6, 90.8, 88.9, 65.1, 14.8; EI-HRMS *m/z* calcd for $C_{28}H_{25}BF_2N_2ONa$ $[M + Na]^+$ 477.1921, found 477.1925.

*4.5.3. BODIPY (**8**).*

A 100 mL round-bottom flask equipped with a magnetic stir bar was charged with **7** (260 mg, 0.57 mmol) and CH_2Cl_2 (50 mL). The resultant solution was cooled to 0 °C using an ice bath. Then DMF (0.5 mL) was added via syringe, followed by PBr_3 (0.86 mL, 1.0 M in CH_2Cl_2). The mixture was allowed to warm to rt without removal of the ice bath, and then it was stirred at rt overnight. The solvent was removed in vacuum. The residue was dissolved in CH_2Cl_2 (10 mL); a white solid that formed was removed by filtration. Silica gel was added to the filtered solution, and after solvent removal, the silica-bound product was purified in a column of silica gel using 5% then 40% ethyl acetate in hexanes as eluent. BODIPY **8** was obtained as an orange solid (256 mg, 0.49 mmol, 87%). FTIR (neat) 3119, 3066, 3034, 2960, 2922, 2851, 2739, 2680, 2347, 2129, 1926, 1546, 1534, 1513, 1498.5, 1460, 1437, 1410, 1363, 1307, 1189, 1154, 1110, 1077, 1051, 974, 818, 762, 703 cm^{-1}; ^1H NMR (400 MHz, $CDCl_3$) δ 7.66 (d, *J* = 8.4 Hz, 2H), 7.53 (d, *J* = 8.4 Hz, 2H), 7.40 (d, *J* = 8.0 Hz, 2H), 7.30 (d, *J* = 8.4 Hz, 2H), 5.99 (s, 2H), 4.51 (s, 2H), 2.56 (s, 6H), 1.43 (s, 6H); ^{13}C NMR (100 MHz, $CDCl_3$) δ 156.0, 143.2, 141.0, 138.4, 135.4, 132.6, 132.2, 131.4, 129.4, 128.5, 124.1, 123.2, 121.6, 90.4, 89.7, 33.1, 14.8; EI-HRMS *m*/*z* calcd for $C_{28}H_{25}BBrF_2N_2$ $[M + H]^+$ 517.1283, found 517.1262.

*4.5.4. Compound (**4**).*

A 50 mL round-bottom flask equipped with a magnetic stir bar was charged with **8** (291 mg, 0.56 mmol), THF (9.0 mL), and 1-methylimidazole (90 μL, 1.12 mmol), in that order. The mixture was stirred at 50 °C overnight. Then the mixture was cooled to rt, and filtered *in vacuo*. The orange solid obtained was washed with Et_2O (5 mL, 4×) and dried under vacuum, to give imidazolium salt **4** as a bright orange solid (326 mg, 0.54 mmol, 97%). FTIR (neat) 3626, 3452, 3381, 3143, 3028, 2975, 2919, 2860, 2727, 2374, 2347, 2217.5, 2035, 1908, 1625, 1616, 1546, 1510, 1466, 1398, 1363, 1304, 1257, 1186, 1157, 1118.5, 1080, 1039, 971, 833, 815, 765, 700

cm^{-1}; ^{1}H NMR (400 MHz, DMSO-d6) δ 9.24 (s, 1H), 7.81 (d, *J* = 8.0 Hz, 2H), 7.73 (s, 2H), 7.66 (d, *J* = 8.0 Hz, 2H), 7.48 (d, *J* = 8.0 Hz, 2H), 7.46 (d, *J* = 8.0 Hz, 2H), 6.21 (s, 2H), 5.48 (s, 2H), 3.87 (s, 3H), 2.46 (s, 6H), 1.39 (s, 6H); ^{13}C NMR (125 MHz, DMSO-d6) δ 155.2, 142.6, 140.9, 136.9, 135.7, 134.5, 132.3, 132.0, 130.4, 128.7, 128.5, 124.1, 122.9, 122.4, 122.3, 121.5, 89.9, 89.4, 51.4, 35.9, 14.2, 14.2; EI-HRMS *m*/*z* calcd for $C_{32}H_{30}BF_2N_4$ $[M - Br]^+$ 519.2518, found 519.2532.

4.6 Synthesis of BODIPY imidazolium salt 5.

*4.6.1. Compound (**10**).*

A 50 mL round-bottom flask equipped with a magnetic stir bar was charged with **9**[23] (260 mg, 0.57 mmol) and CH_2Cl_2 (15 mL). The resultant solution was cooled to 0 °C using an ice bath. DMF (0.15 mL) was added *via* syringe, followed by PBr_3 (0.63 mL, 1.0 M in CH_2Cl_2). The mixture was allowed to warm to rt without removal of the ice bath, and then it was stirred at rt overnight. The solvent was removed *in vacuo*. The residue was dissolved in ethyl acetate (20 mL) and water (20 mL). The aqueous layer was extracted with ethyl acetate (3 ×). The combined organic layers were dried over $MgSO_4$ and filtered, and the solvent was removed from the filtrate *in vacuo* to afford the crude product as an orange solid. Purification was done by column chromatography on silica gel using 20% ethyl acetate in hexanes as the eluent. Compound **10** was obtained as a bright orange solid (106 mg, 0.25 mmol, 61%). FTIR (neat) 3101, 3039.5, 2978, 2963, 2927.5, 2863, 2730, 2677, 2497, 2377, 2347, 2306, 2123, 1728, 1625, 1613.5, 1540, 1501.5, 1469, 1437, 1407, 1366, 1304, 1263, 1180, 1151, 1048, 965, 809, 753, 709 cm^{-1}; ^{1}H NMR (400 MHz, $CDCl_3$) δ 7.50 (d, *J* = 8.0 Hz, 2H), 7.28 (d, *J* = 8.0 Hz, 2H), 5.98 (s, 2H), 4.82 (d, *J* = 3.2 Hz, 2H), 2.56 (s, 6H), 1.39 (s, 6H); ^{13}C NMR (100 MHz, $CDCl_3$) δ 155.9, 143.2,

141.1, 139.3, 135.3, 131.5, 130.0, 128.7, 121.5, 32.8, 14.8, 14.7; EI-HRMS *m*/*z* calcd for $C_{20}H_{20}BBrF_2N_2Na$ $[M + Na]^+$ 439.0784, found 439.0767.

*4.6.2. Compound (**5**).*

A 25 mL round-bottom flask equipped with a magnetic stir bar was charged with **10** (208 mg, 0.50 mmol), THF (8.0 mL), and 1-methylimidazole (80 μL, 1.00 mmol), in that order. The mixture was stirred at 50 °C overnight. Then the mixture was cooled to rt and filtered to recover the precipitate. The orange solid obtained was washed with Et_2O (5 mL, 4×) and dried under vacuum to give imidazolium salt **5** as a bright orange solid (247 mg, 0.49 mmol, 99%). FTIR (neat) 3458, 3381, 3143, 3095.5, 2983.5, 2922, 2374, 2344, 2026, 1622, 1546, 1501.5, 1463, 1410, 1369, 1307, 1180, 1148, 1051, 974, 847, 803, 762, 730 cm^{-1}; ^1H NMR (400 MHz, DMSO-d6) δ 9.26 (s, 1H), 7.75 (s, 2H), 7.55 (d, *J* = 7.6 Hz, 2H), 7.46 (d, *J* = 7.2 Hz, 2H), 6.18 (s, 2H), 5.55 (s, 2H), 3.89 (s, 3H), 2.45 (s, 6H), 1.31 (s, 6H); ^{13}C NMR (100 MHz, DMSO-d6) δ 155.1, 142.6, 141.2, 137.0, 136.0, 134.3, 130.6, 128.8, 128.5, 124.2, 122.2, 121.5, 51.4, 36.0, 14.2, 14.1; EI-HRMS *m*/*z* calcd for $C_{24}H_{26}BF_2N_4$ $[M - Br]^+$ 419.2219, found 419.2217.

4.7 Synthesis of BODIPY-tagged ROMP catalyst 11.

*4.7.1. BODIPY (**12**).*

See the general procedure for the Pd/Cu coupling reaction. The materials used were BODIPY **6**[21] (349 mg, 0.77 mmol), 4-ethynylbenzoic acid[26] (170 mg, 1.16 mmol), $PdCl_2(PPh_3)_2$ (27.0 mg, 38.0 μmol), CuI (15.0 mg, 77.0 μmol), TEA (5.0 mL), and THF (15.0 mL) at rt overnight. The crude product (348 mg), pentafluorophenol (135 mg, 0.73 mmol), DMAP (5 mg, 0.04 mmol), and DCC (224 mg, 1.08 mmol) were added to a 50 mL round-bottom flask equipped with a magnetic stir bar. CH_2Cl_2 (12 mL) was added *via* syringe, and the mixture was stirred overnight at rt. The solvent was removed *in vacuo*, and the residue was purified on a silica gel

column using 5%, then 30% ethyl acetate in hexanes. Pentafluorophenol ester **12** was obtained as an orange solid (316 mg, 0.50 mmol, 65% over two steps). FTIR (neat) 3499, 3361, 3101, 2998, 2954, 2925, 2857, 2733, 2668, 2462, 2347, 2220, 1761, 1540, 1513, 1463, 1404, 1372, 1298, 1236, 1186, 1151, 1077, 1045, 974, 824, 709 cm^{-1}; ^{1}H NMR (400 MHz, $CDCl_3$) δ 8.21 (d, *J* = 8.0 Hz, 2H), 7.72 (d, *J* = 8.4 Hz, 4H), 7.34 (d, *J* = 8.0 Hz, 2H), 6.01 (s, 2H), 2.57 (s, 6H), 1.44 (s, 6H); ^{13}C NMR (125 MHz, $CDCl_3$) δ 162.2, 156.1, 143.1, 140.7, 136.0, 132.8, 132.2, 131.3, 130.9, 129.7, 128.6, 126.6, 123.4, 121.6, 93.0, 89.7, 14.8. The chemical shifts of the four different types of carbons on the C_6F_5 ring are not reported because the extensive one-bond and long-range $^{13}C-^{19}F$ couplings make the individual signals too weak and broad to interpret with any confidence. EI-HRMS *m*/*z* calcd for $C_{34}H_{22}BF_7N_2O_2Na$ $[M + Na]^+$ 657.1588, found 657.1561.

4.7.2. BODIPY –tagged ROMP catalyst (***11*).**

Inside a nitrogen-filled glove box, a 10 mL round-bottom flask equipped with a magnetic stir bar was charged with **13**[29] (50 mg, 66 μmol). CH_2Cl_2 (3 mL) was added and the flask was capped with a septum. The seal of the septum was reinforced with Teflon tape and the flask was taken out of the glove box. Hydrogen chloride was bubbled into the flask for 1 h. The HCl was generated by dropwise addition of conc. H_2SO_4 to NH_4Cl. Then the mixture was stirred 2 h at rt. The solvent was removed by rotary evaporation. Next, the flask was charged with BODIPY **12**. Under a nitrogen atmosphere, DMF (2.5 mL) and Et_3N (0.2 mL) were added, and the mixture was stirred at rt overnight. The solvent was removed *in vacuo* (using a Schlenk line with a dry ice trap, not by rotary evaporation) at 40 °C. The residue was dissolved in degassed CH_2Cl_2 and purified under ~ anaerobic conditions[23] using a silica gel column (Geduran, see General Methods). In ~ anaerobic chromatography, the column was packed under a stream of nitrogen,

and the solvents used as eluents (diethyl ether and pentane) were degassed prior to use with a sparge of nitrogen for 30 min. The product was eluted under nitrogen and it was collected in a round-bottom flask previously purged with nitrogen and equipped with a magnetic stir bar and a nitrogen sparge. The eluant was removed using a Schlenk line with a dry ice trap (not by rotary evaporation). Unreacted BODIPY **12** was removed using 50% distilled Et_2O in pentane, then pure Et_2O was used to elute the desired product. Complex **11** was obtained as a dark brown solid (56 mg, 50 μmol, 77%). FTIR (neat) 3343, 2963, 2922, 2854, 2733, 2379.5, 2344, 2321, 2049.5, 1979, 1946, 1923, 1840, 1554, 1475, 1440, 1398, 1378, 1310, 1263, 1198, 1157, 1083, 983, 853 cm^{-1}; ^1H NMR (500 MHz, CD_2Cl_2) δ 16.40 (s, 1H), 7.76 (br s, 2H), 7.69 (d, *J* = 6.8 Hz, 2H), 7.57 (d, *J* = 7.2 Hz, 3H), 7.33 (d, *J* = 6.8 Hz, 2H), 7.16 (br s, 1H), 7.10 (br s, 1H), 7.08 (br s, 1H), 6.99−6.98 (m, 1H), 6.92 (d, *J* = 5.2 Hz, 2H), 6.87 (d, *J* = 6.4 Hz, 1H), 6.03 (s, 2H), 4.94 (m, 1H), 4.68 (br s, 1H), 4.32 (t, *J* = 8.8 Hz, 1H), 3.95 (dd, J_1 = 6.4 Hz, J_2 = 8.8 Hz, 2H), 3.68 (br s, 1H), 2.90−2.80 (br m, 3H), 2.52 (s, 6H), 2.41 (br m, 15H), 1.45 (s, 6H), 1.28 (br d, *J* = 8.8 Hz, 6H); ^{13}C NMR (125 MHz, CD_2Cl_2) δ 297.1, 216.1, 167.3, 156.2, 152.6, 145.5, 143.8, 141.5, 139.9, 139.7, 135.8, 133.9, 133.0, 132.1, 131.7, 131.0, 130.5, 130.4, 130.1, 128.9, 127.9, 126.7, 124.2, 122.9, 122.8, 121.8, 113.5, 91.4, 90.2, 75.7, 64.2, 42.7, 21.5, 21.4, 14.8; MALDI-TOF MS (+eV) *m*/*z* calcd for $C_{60}H_{63}BCl_2F_2N_5O_2Ru$ 1106.9, found 1106.5.

Acknowledgments

The NSF (CHE-1007483) provided financial support. S. L. acknowledges support from the Robert A. Welch Foundation (C-1664). We thank Drs. I. Chester of FAR Research, Inc., and R. Awartari of Petra Research, Inc., for providing trimethylsilylacetylene that was used to make some of the starting alkynes.

Supplementary data

Experimental procedures and spectroscopic results supplied as supplemental data.

5. References

(1) Yurke, B.; Turber, A.; Mills, A. P.; Simmel, F. C.; Neumann, J. L. *Nature* **2000**, *406*, 605- 608.

(2) Boyer, P. D. *Angew. Chem. Int. Ed.* **1998,** *37, 2296-2307.*

(3) Carter, N. J.; Cross, R. *Nature* **2005**, *435*, 308–312.

(4) Konstas, K.; Langford, S. J.; Latter, M. J. *Int. J. Mol. Sci.* **2010**, *11*, 2453– 2472.

(5) Shirai, Y.; Morin, J.-F.; Sasaki, T.; Guerrero, J. M.; Tour, J. M. *Chem. Soc.Rev.* **2006**, *35*, 1043–55.

(6) Vives, G.; Tour, J. M. *Acc. Chem. Res.* **2009,** *42*, 473–487.

(7) Morin, J.-F.; Shirai, Y.; Tour, J. M. *Org. lett.* **2006**, *8*, 1713–1716.

(8) Chiang, P.-T.; Mielke, J.; Godoy, J.; Guerrero, J. M.; Alemany, L. B.; Villagomez, C. J.; Saywell, A.; Grill, L.; Tour, J. M. *ACS Nano* **2012**, *6*, 592-597.

(9) Godoy, J.; Vives, G.; Tour, J. M. *ACS Nano* **2011**, *5*, 85–90.

(10) (a) Laocharoensuk, R.; Burdick, J.; Wang, J. *ACS Nano* **2008**, *2*, 1069−1075. (b) Paxton, W. F.; Kistler, K. C.; Olmeda, C. C.; Sen, A.; Angelo, S. K.; Cao, Y.; Mallouk, T. E.; Lammert, P. E.; Crespi, V. H. *J. Am. Chem. Soc.* **2004**, *126*, 13424−13431. (c) Manesh, K. M.; Cardona, M.; Yuan, R.; Clark, M.; Kagan, D.; Balasubramanian, S.; Wang, J. *ACS Nano* **2010**, *4*, 1799−1804.

(11) Heureux, N.; Lusitani, F.; Browne, W. R.; Pshenichnikov, M. S.; van Loosdrecht, P. H. M.; Feringa, B. L. *Small* **2008**, *4*, 476−480.

(12) Smith, G. A.; Portnoy, D. A. *Trends Microbiol.* **1997**, 5, 272-276.

(13) Pavlick, R. A.; Sengupta, S.; McFadden, T.; Zhang, H.; Sen, A. *Angew. Chem., Int. Ed.* **2011**, *50*, 9374-9377

(14) Solovev, A. A.; Sanchez, S.; Schmidt, O. G. *Nanoscale* **2013**, *5*, 1284-1293.

(15) Pavlick, R. A.; Dey, K. K.; Sirjoosingh, A.; Benesi, A.; Sen, A. *Nanoscale* **2013**, *5*, 1301-1304.

(16) Tcherniak, A.; Reznick, C.; Link, S.; Landes, C. F. *Anal. Chem.* **2009**, *81*, 746−754.

(17) Samojlowicz, C.; Bieniek, M.; Grela, K. *Chem. Rev.* **2009**, *109*, 3708−3742.

(18) Deshmukh, P. H.; Blechert, S. *Dalton Trans.* **2007**, 2479–2491.

(19) (a) Treibs, A.; Kreuzer, F.–H. *Liebigs Ann. Chem.* **1968**, *718*, 208−223. b) Loudet, A.; Burgess, K. *Chem. Rev.* **2007**, *107*, 4891−4932.

(20) Kingsbury, J. S.; Harrity, J. P. A.; Bonitatebus, P. J.; Hoveyda, A. H. *J. Am. Chem. Soc.* **1999**, *121*, 791–799.

(21) Godoy, J.; Vives, G.; Tour, J. M. *Org. Lett.* **2010**, *12*, 1464−1467.

(22) Percec, V.; Rudick, J. G.; Peterca, M.; Wagner, M.; Obata, M.; Mitchell, C. M.; Cho, W.−D.; Balagurusamy, V. S. K.; Heiney, P. A. *J. Am. Chem. Soc.* **2005**, *127*, 15257−15264.

(23) Yue, Y.; Guo, Y.; Xu, J.; Shao, S. *New J. Chem.* **2011**, *35*, 61−64. For full characterization of **9** see: Matsumoto, T.; Urano, Y.; Takahashi, Y.; Mori, Y.; Terai, T.; Nagano, T.; *J. Org. Chem.* **2011**, *76*, 3616−3625.

(24) Vougioukalakis, G. C.; Grubbs, R. H. *Chem. Rev.* **2010**, *110*, 1746−1787.

(25) Weskamp, T.; Kohl, F. J.; Herrman, W. A. *J. Organomet. Chem.* **1999**, *582*, 362-365.

(26) Jones, L. F.; Cochrane, M. E.; Koivisto, B. D.; Leigh, D. A.; Perlepes, S. P.; Wernsdorfer, W.; Brechin, E. K. *Inorg. Chim. Acta* **2008**, *361*, 3420−3426.

(27) Lo, C.; Ringenberg, M. R.; Gnandt, D.; Wilson, Y.; Ward, T. R. *Chem. Comm.* **2011**, *47*, 12065−12067

(28) Chen, J.; Burghart, A.; Wan, C-W.; Thai, L.; Ortiz, C.; Reibenspies, J.; Burgess, K. *Tetrahedron Lett*. **2000**, *41*, 2303−2307.

(29) Kim, K. H.; Ok, T.; Lee, K.; Lee, H.-S.; Chang, K. T.; Ihee, H.; Sohn, J.-H.; *J. Am. Chem. Soc.* **2010**, *132*, 12027−12033.

(30) (a) Garber, S. B.; Kingsbury, J. S.; Gray, B. L.; Hoveyda, A. H. *J. Am. Chem. Soc.* **2000**, *122*, 8168-8179. (b) Gessler, S.; Randl, S.; Blechert, S. *Tetrahedron Lett.* **2000**, *41*, 9973-9976.

(31) Ritter, T.; Hejl, A.; Wenzel, A. G.; Funk, T. W.; Grubbs, R. H. *Organometallics* **2006**, *25*, 5740–5745.

Synthesis of a Fluorescent BODIPY-tagged ROMP catalyst and Initial Polymerization-Propelled Diffusion Studies—Supplemental Data

Jazmin Godoy,[1] Víctor García-López,[1] Lin-Yung Wang,[1] Simon Rondeau-Gagné,[1,2] Stephan Link,[1,3] Angel A. Martí,[1,3,4]* and James M. Tour[1,3,4]*

[1]Department of Chemistry, Rice University, 6100 Main Street, Houston, Texas 77005

[3]Smalley Institute for Nanoscale Science and Technology, Rice University, 6100 Main Street, Houston, Texas 77005

[4]Department of Materials Science and NanoEngineering, Rice University, 6100 Main Street, Houston, Texas 77005

[2]Université Laval, Département de Chimie, Pavillon Alexandre-Vachon Bureau 1407, Laval, Canada 4137

Corresponding author

* (A. M.) E-mail: amarti@rice.edu

*(J.M.T) E-mail: tour@rice.edu

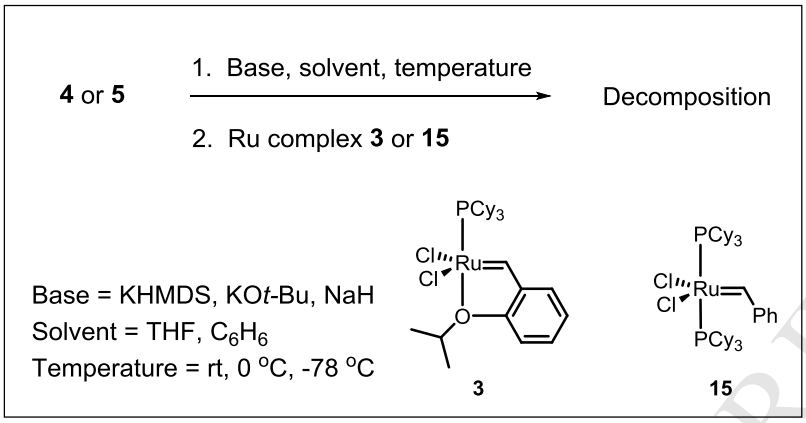

Figure S1. Failed approach to synthesize BODIPY-tagged Hoveyda-Grubbs catalysts **1** and **2**.

Table S1. ROMP of cod catalyzed by **11.**

Time (min)	% conversion
4.2	96.8
5.2	98.9
6.4	99.6
7.4	99.8
8.6	99.9
9.6	99.9
10.8	99.9
11.8	99.9

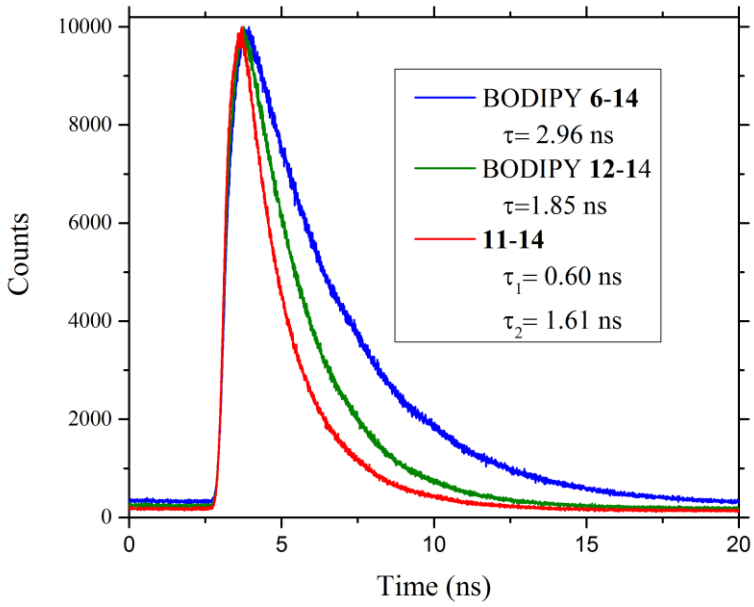

Figure S2. Time resolved fluorescence decay for (1:5) mixtures of BODIPY **6-14**, **11-14,** and **12-14** in CH_2Cl_2.

Optical Setup for FCS. FCS was performed using a home-built inverted confocal microscope (Observer.D1, Zeiss). The light from a 532 nm laser (Verdi-6, Coherent Inc.) was collimated and expanded to overfill the back aperture of the microscope objective (Fluar, Zeiss; 100×, NA = 1.3). The beam was circularly polarized using a λ/4 waveplate (Newport). The laser power was attenuated to ~ 150 nW using neutral density filters (Thorlabs). This power gives a signal to background ratio of ~ 10, yet ensured negligible heating of the sample. The focal plane of the objective was set to approximately ~ 6 μm inside the solution to avoid excessive scattered light from the glass−water interface. Polystyrene fluorospheres (100 nm in diameter, Molecular Probes) were used for alignment and calibration of the focal volume. The fluorescence was collected in the backward direction and redirected to a 50 μm pinhole (Thorlabs) before focusing onto an avalanche photodetector (SPCM-AQRH, Perkin-Elmer).

Calculation of Diffusion Constants using FCS. FCS records the fluorescence fluctuations from a single light-emitting source in a small volume and transforms the time traces into autocorrelation curves via the correlation analysis. The intensity of the autocorrelation as a function of lagtime (τ) can be expressed in terms of experimental parameters as in eq 2:

$$G(\tau) = \frac{1}{V_{eff}<C>} \cdot \frac{1}{\left(1+\frac{\tau}{\tau_D}\right)} \cdot \frac{1}{\left(1+\left(\frac{r_0}{z_0}\right)^2\left(\frac{\tau}{\tau_D}\right)\right)^{1/2}} \quad (2)$$

where V_{eff} is the volume, r_0 is the beam waist, z_0 is the beam height, τ_D is the characteristic diffusion time, and $<C>$ is the analyte concentration. The experimental characteristic diffusion time can thus be obtained by fitting the autocorrelation curves with the above equation. Finally, the three-dimensional diffusion coefficient D can be calculated using eq 3:

$$\tau_D = \frac{r_0^2}{4D_t} \quad (3)$$

To avoid potential decomposition of **12** due to oxygen and/or moisture a non-fluorescent ROMP catalyst was added to serve as a sacrificial substrate to oxygen and/or moisture. The second generation Hoveyda-Grubbs catalyst (**14**) was chosen, since its catalytic activity is very similar that of **11**. The composition of the FCS sample was therefore: 0.47 mM of **14**, 20 nM of **11**, and for the polymerization experiments, 0.47 M of cod.

To assess the impact of the viscosity increase on the diffusion of **11**, the diffusion of BODIPY **6** was studied. The FCS sample contained 0.47 mM of **14**, ~ 1 nM of BODIPY **6**, and for the polymerization experiments, 0.47 M of cod. As expected, the diffusion coefficient of **6** decreased; before adding cod, Dt = (1.42 ± 0.28) x 10^{-10} m^2/s, but upon addition of cod Dt dropped to (0.75 ± 0.13) x 10^{-10} m^2/s. A correction factor was defined as the ratio of the diffusion coefficients of the BODIPY **6** after and before adding COD. In this process,

the change in diffusion coefficient is entirely due to the change in viscosity as a result of the polymerization reaction products. We then divided the measured diffusion coefficients of BODIPY **11** + cod by this correction factor. Using these data to correct the diffusion due to the increase in viscosity, there was an apparent increase in the diffusion coefficient of **11** during the ROMP process.

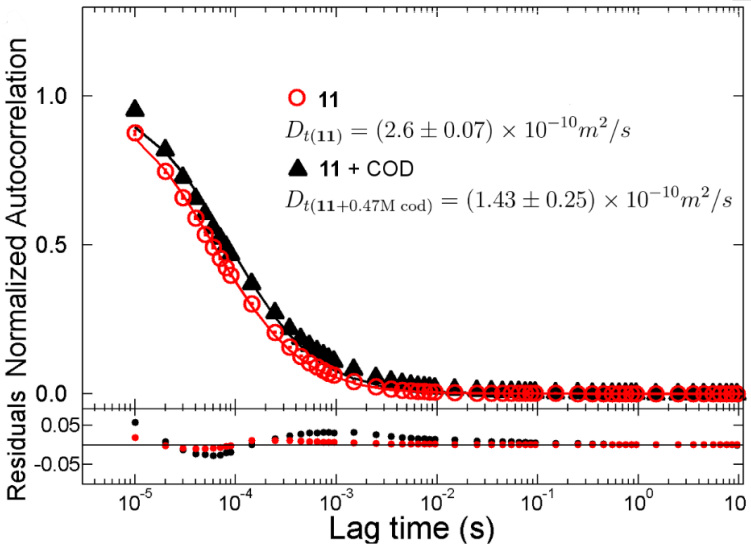

Figure S3. Autocorrelation curves of **11** as a 20 nM solution in IPA, before (red) and after addition of cod (black).

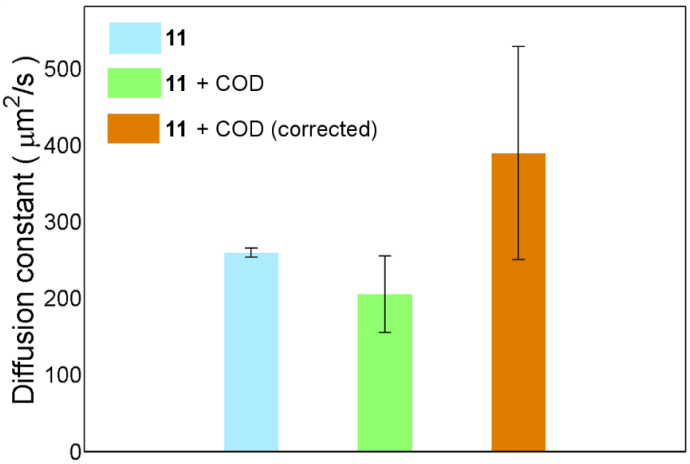

Figure S4. Effect of adding cod on the diffusion coefficient of **11** in IPA. The data in orange was calculated from the data in green after correcting for the viscosity change caused by the polymerization reaction using BODIPY as a probe. The error bars correspond to the standard deviation of the data.

Figure S3 ^{1}H NMR spectrum of 4-ethynyl benzyl alcohol (400 MHz, $CDCl_3$).

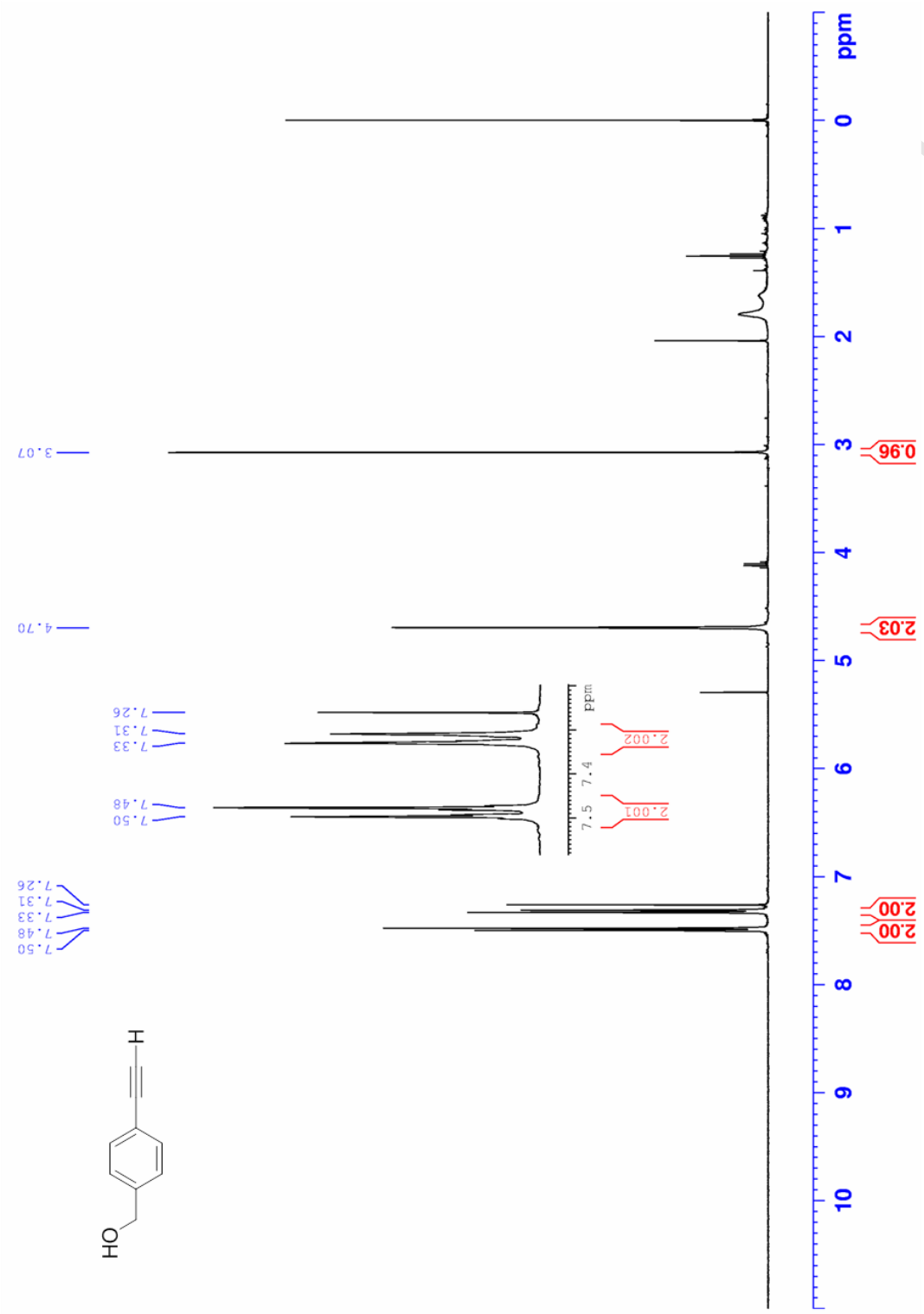

Figure S4. ^{1}H NMR spectrum of BODIPY **7** (400 MHz, $CDCl_3$).

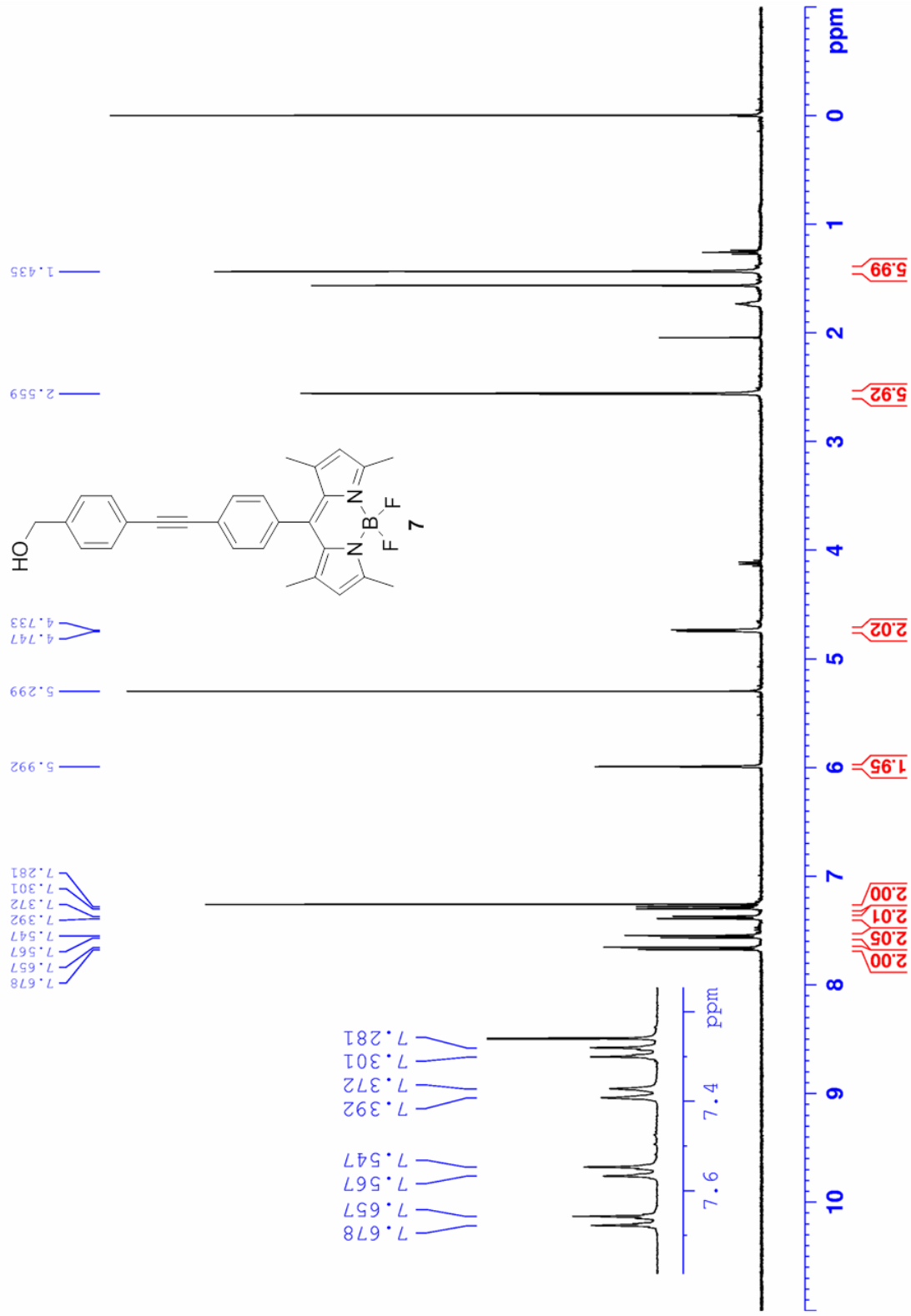

Figure S5. ^{13}C NMR spectrum of BODIPY **7** (100 MHz, $CDCl_3$).

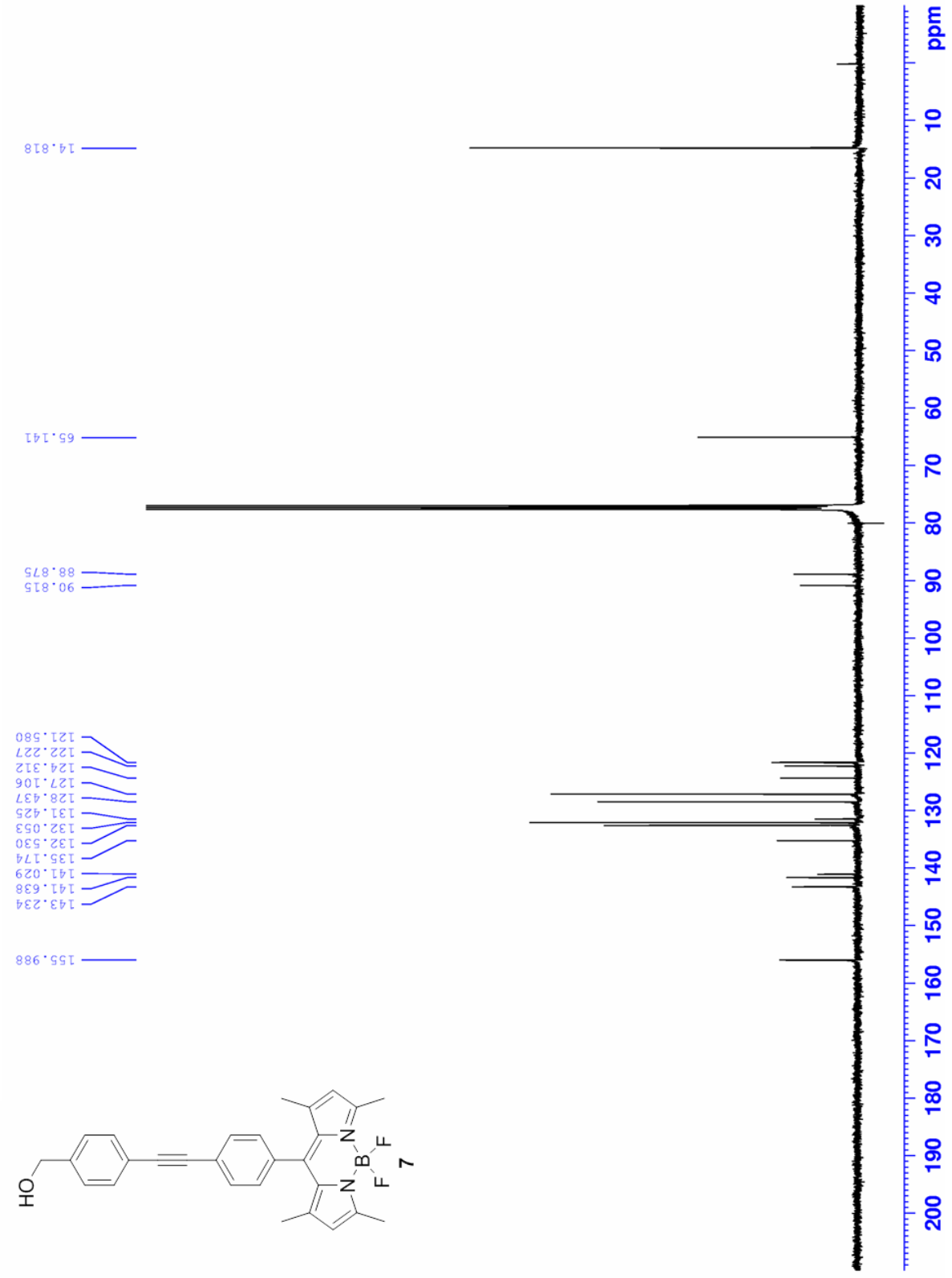

Figure S6. ^{1}H NMR spectrum of BODIPY **8** (400 MHz, CDCl3).

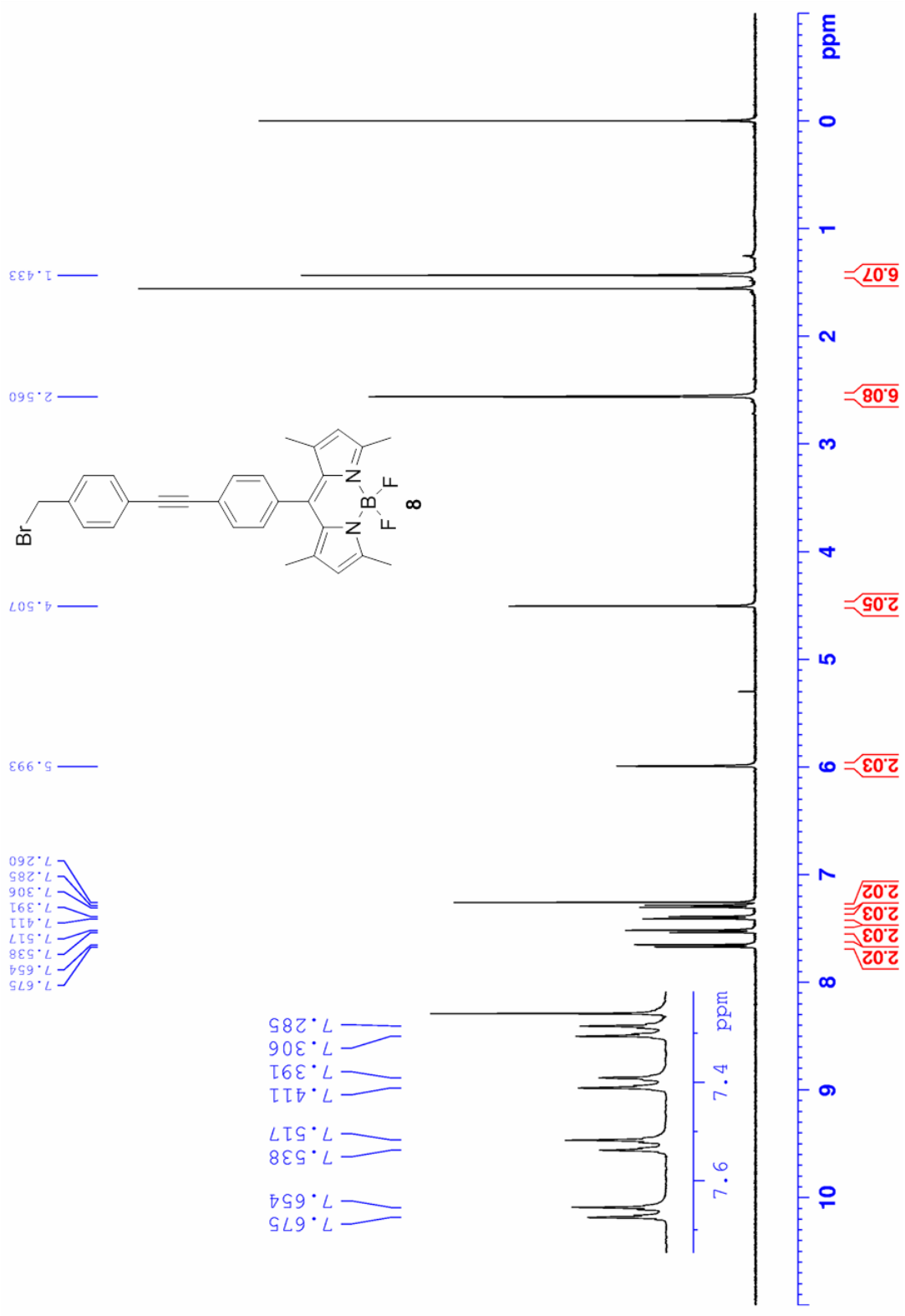

Figure S7. ^{13}C NMR spectrum of BODIPY **8** (100 MHz, $CDCl_3$).

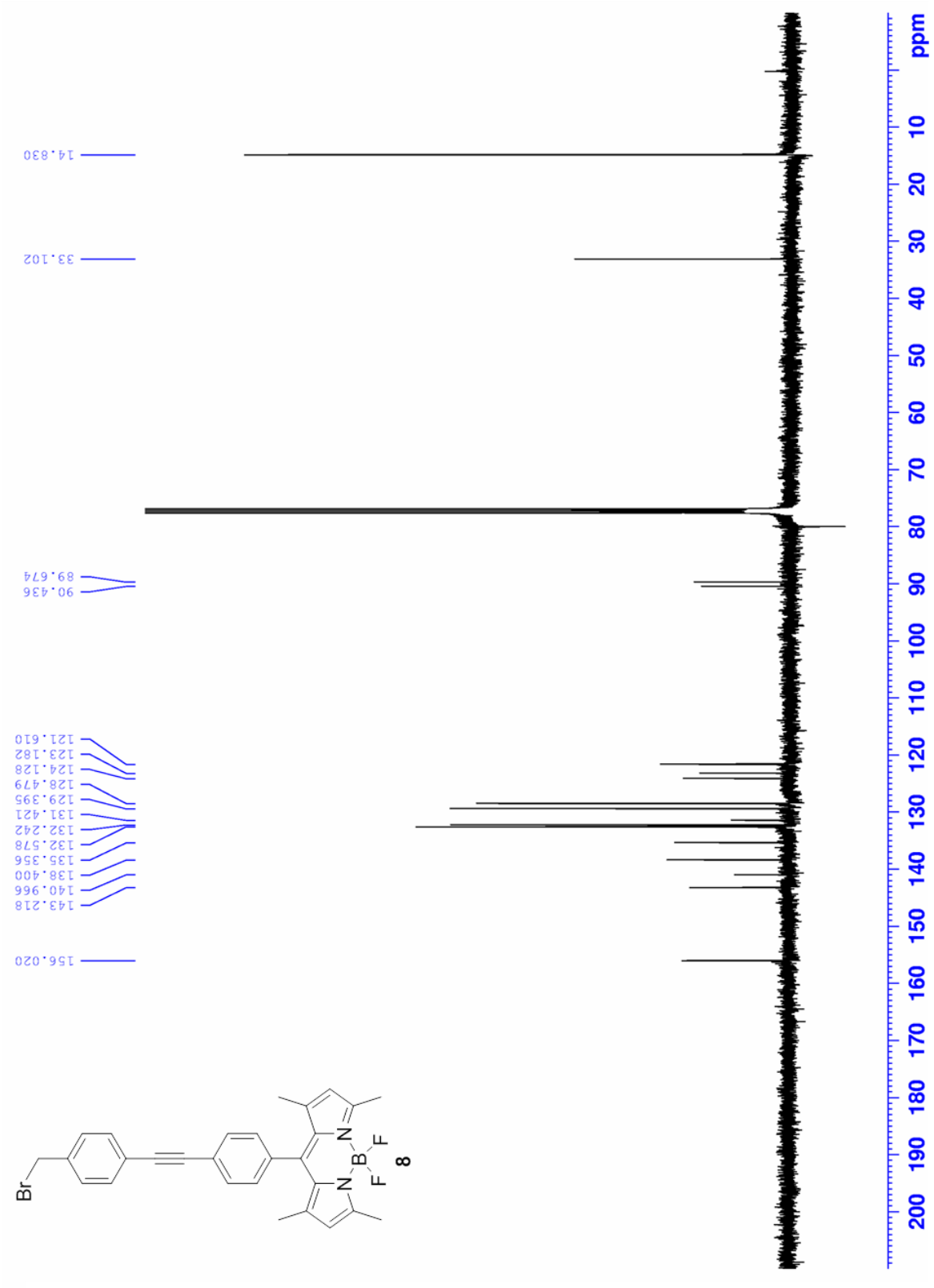

Figure S8. ^{1}H NMR spectrum of **4** (400 MHz, DMSO-d6).

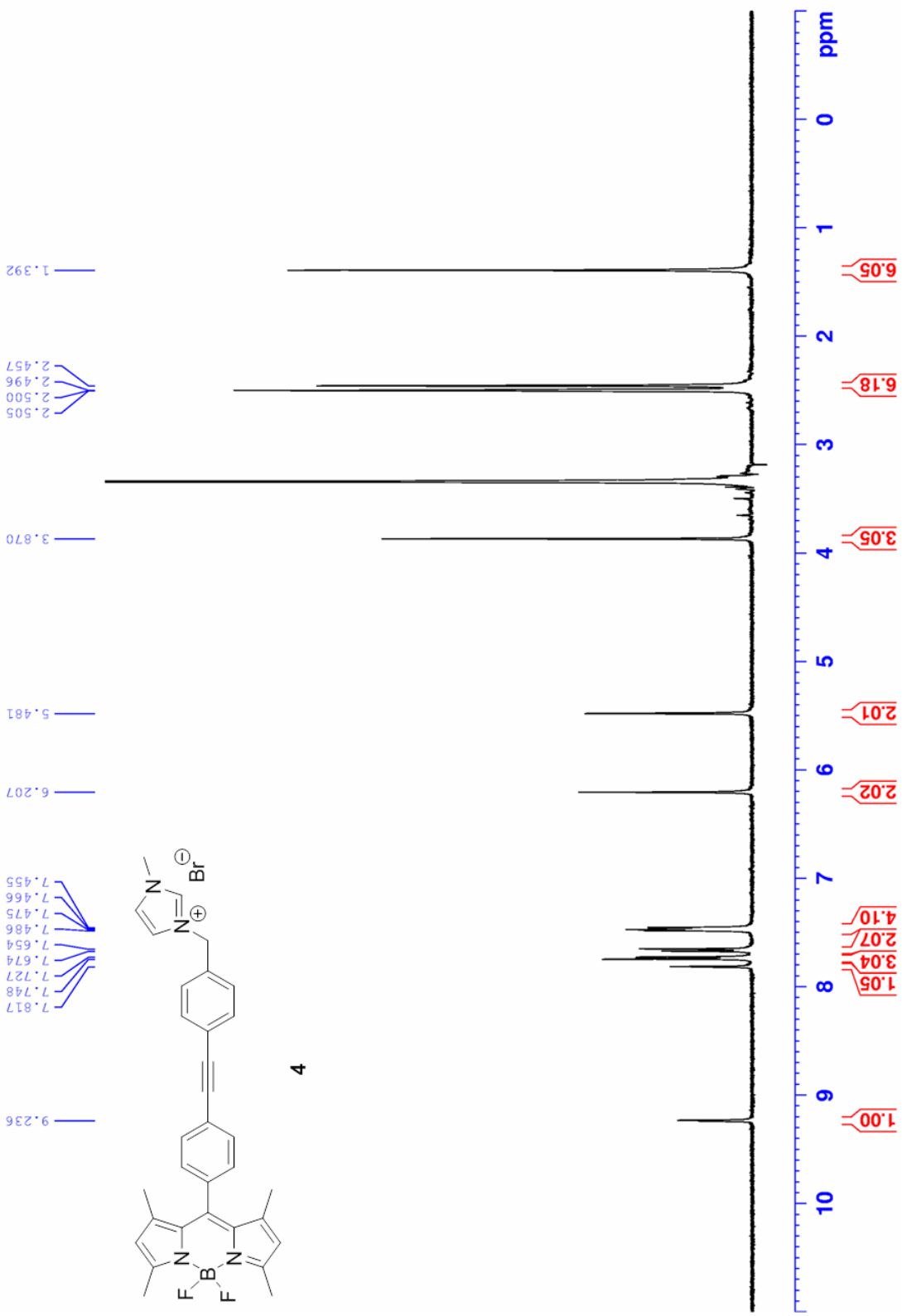

Figure S9. ^{13}C NMR spectrum of **4** (125 MHz, DMSO-d6).

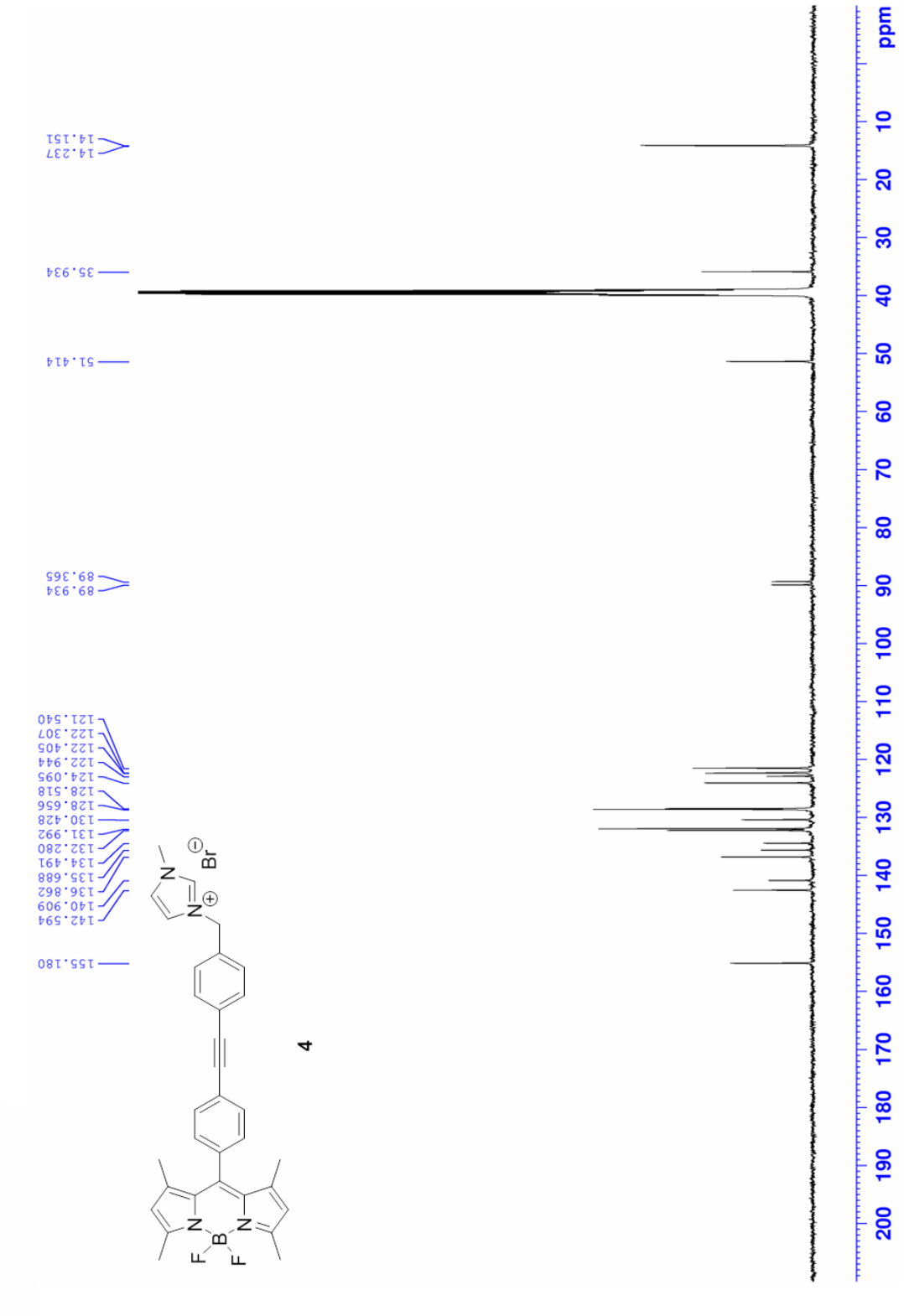

Figure S10. ^{1}H NMR spectrum of BODIPY **10** (400 MHz, $CDCl_3$).

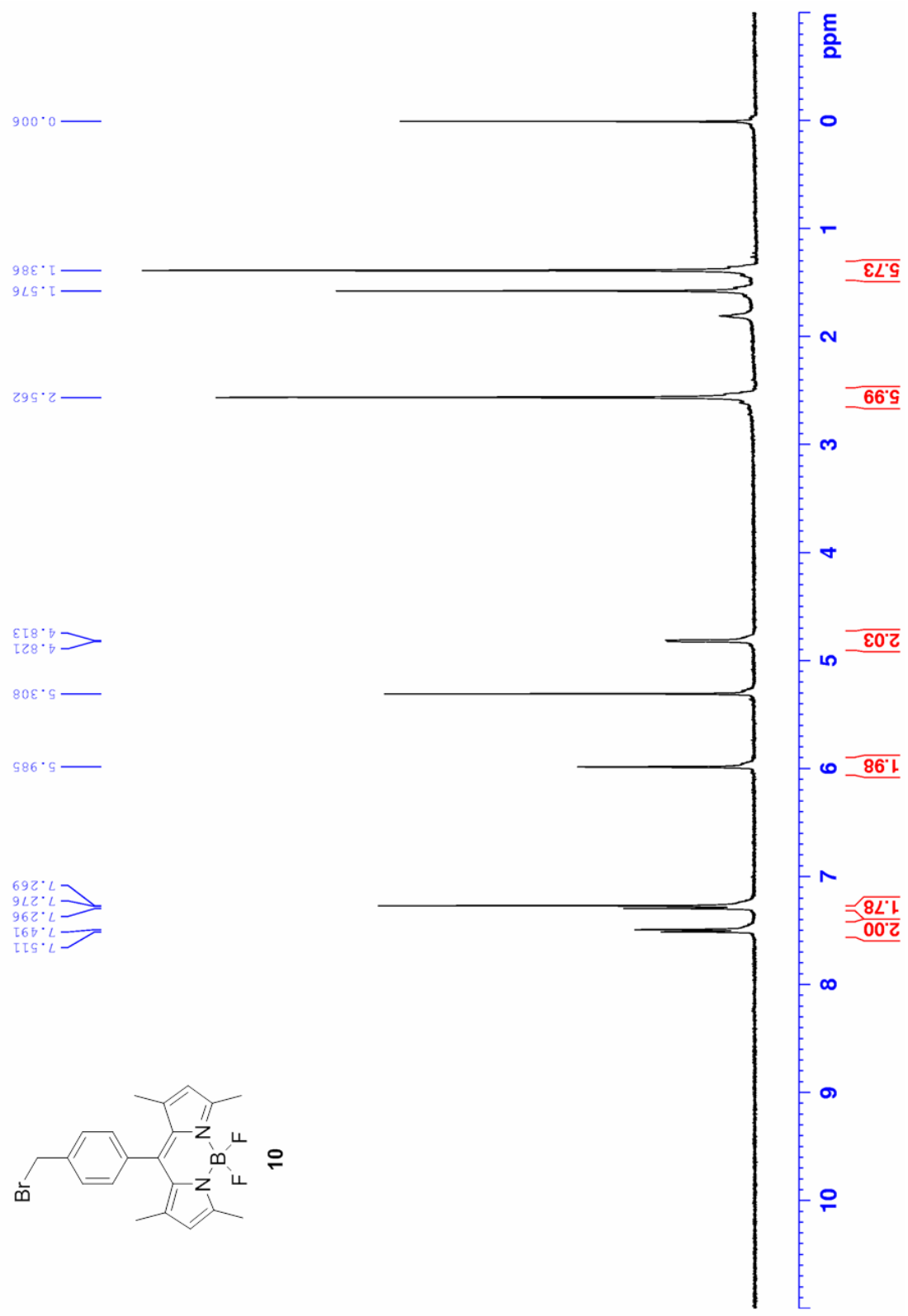

Figure S11. ^{13}C NMR spectrum of BODIPY **10** (100 MHz, $CDCl_3$).

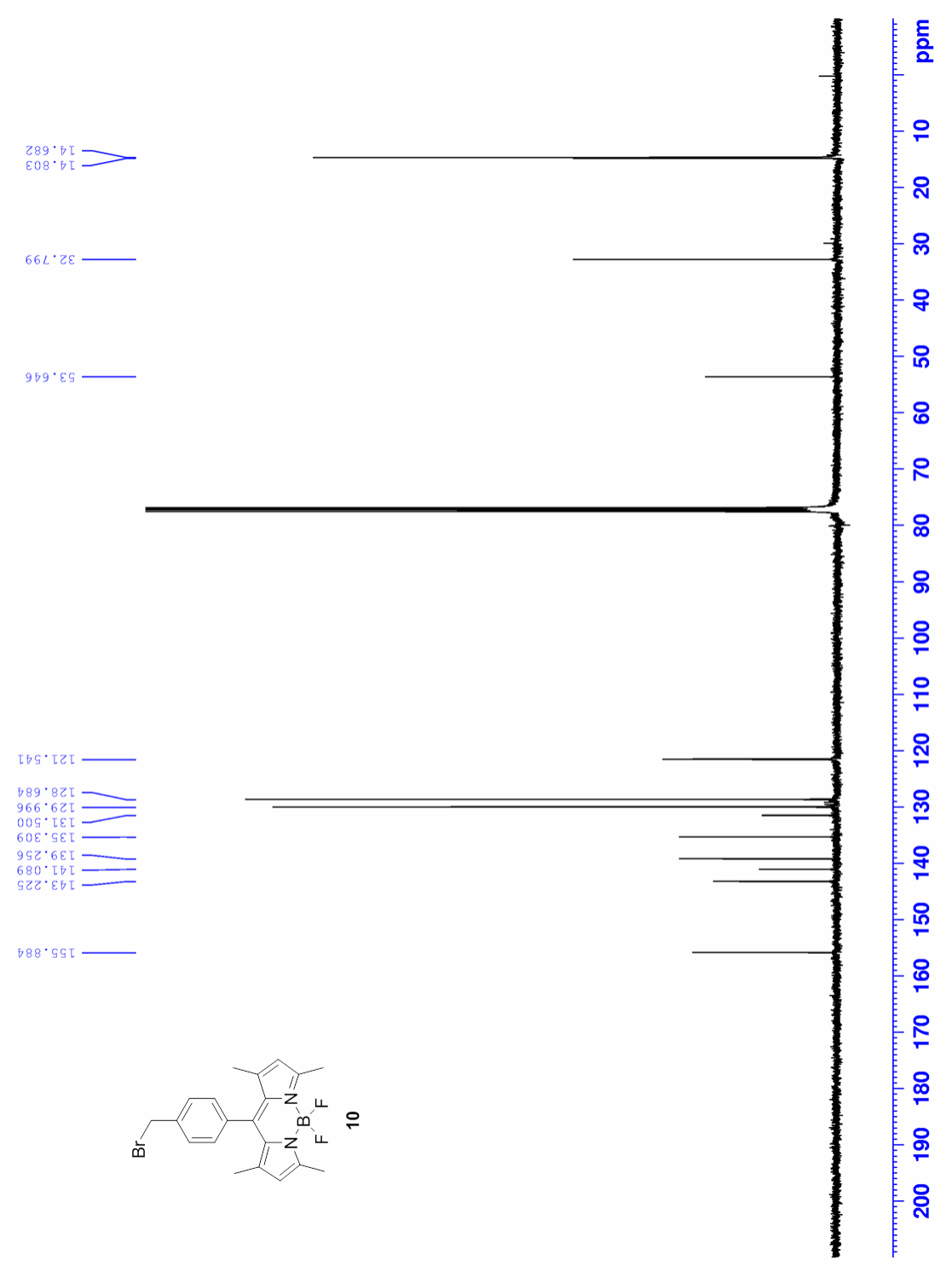

Figure S12. ^{1}H NMR spectrum of **5** (400 MHz, DMSO-d6).

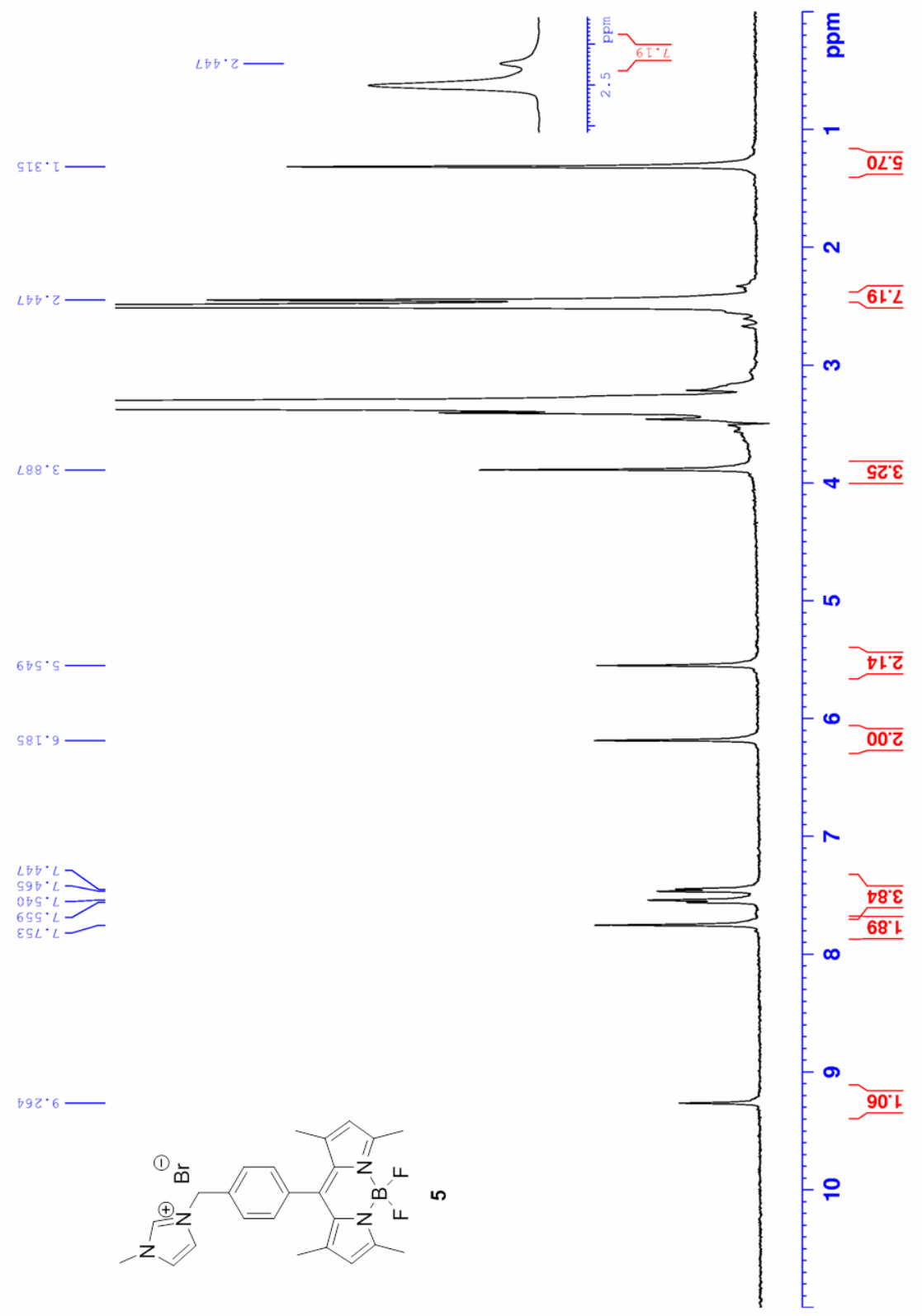

Figure S13. ^{13}C NMR spectrum of **5** (100 MHz, DMSO-d6).

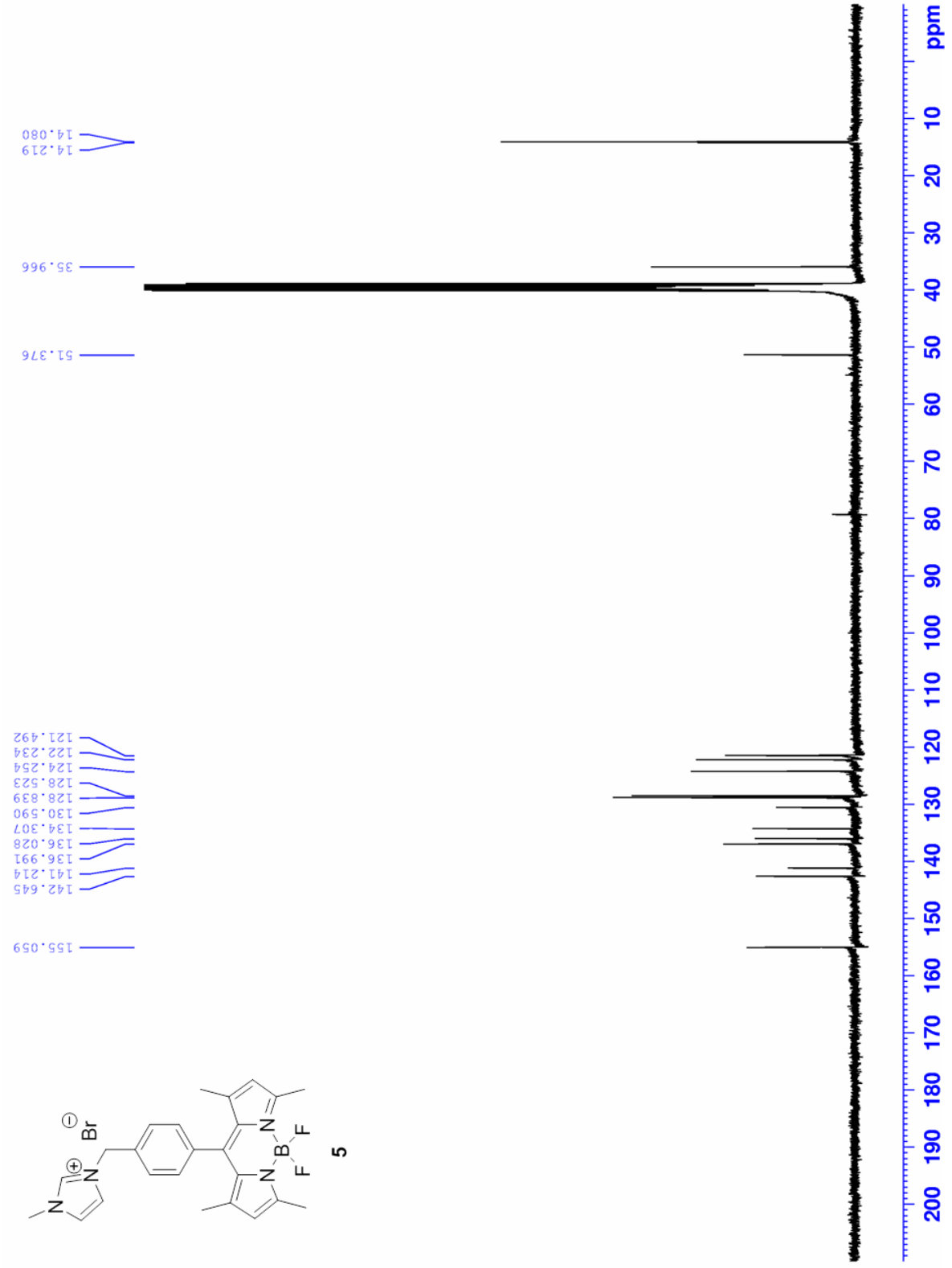

Figure S14. ^{1}H NMR spectrum of **12** (400 MHz, $CDCl_3$).

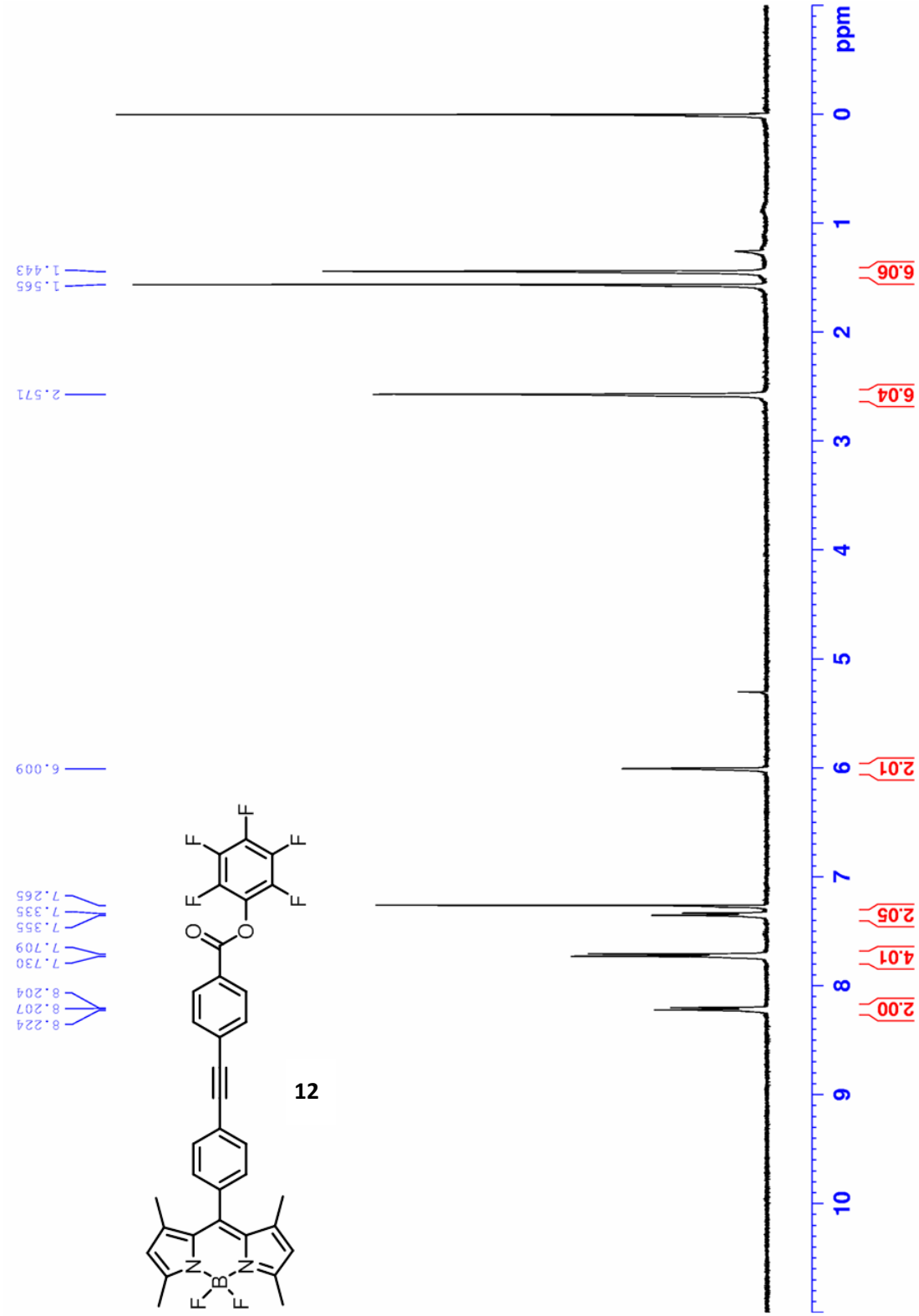

Figure S15. ^{13}C NMR spectrum of **12** (125 MHz, CDCl3).

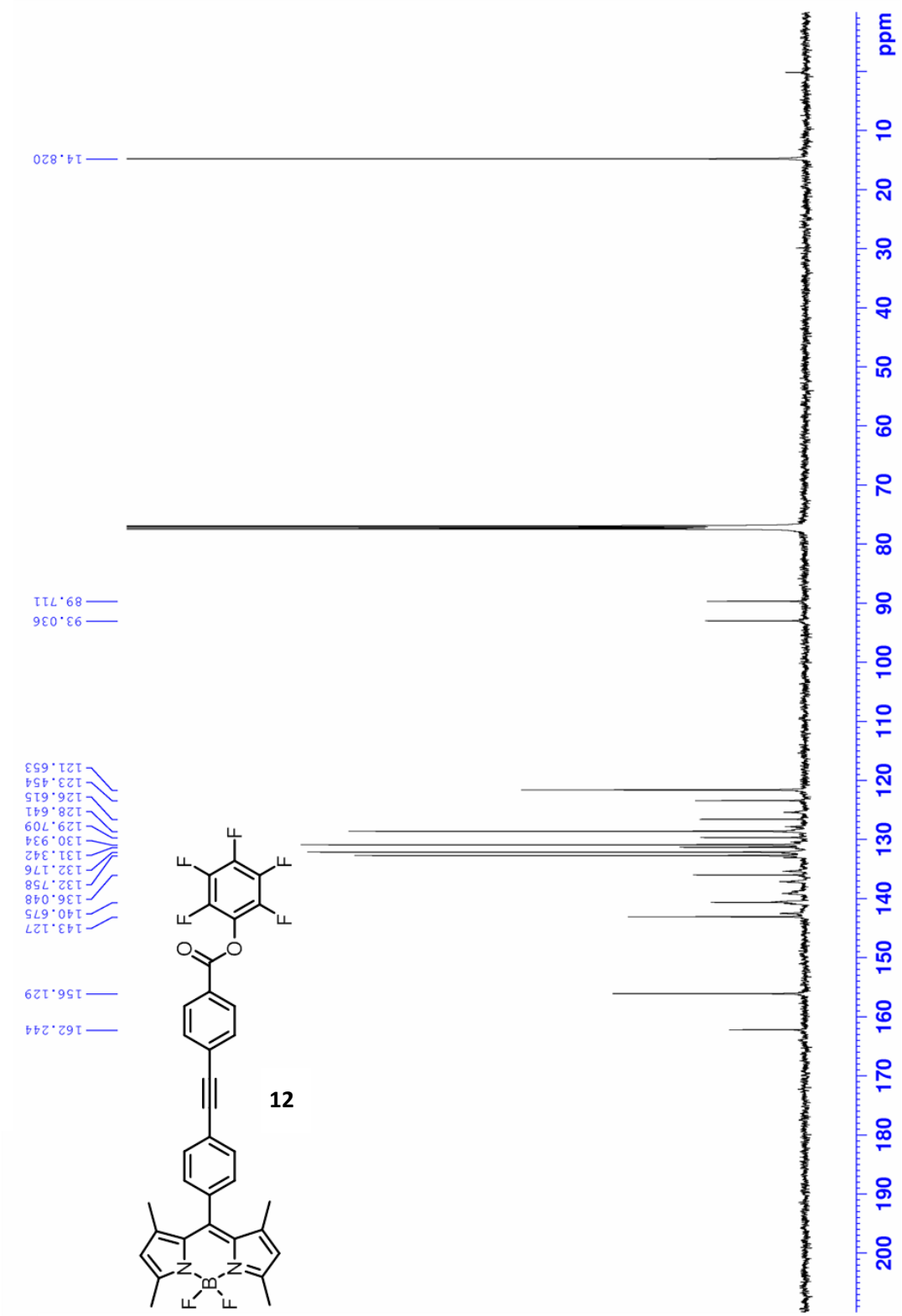

Figure S16. ^{1}H NMR spectrum of **11** (500 MHz, CD_2Cl_2).

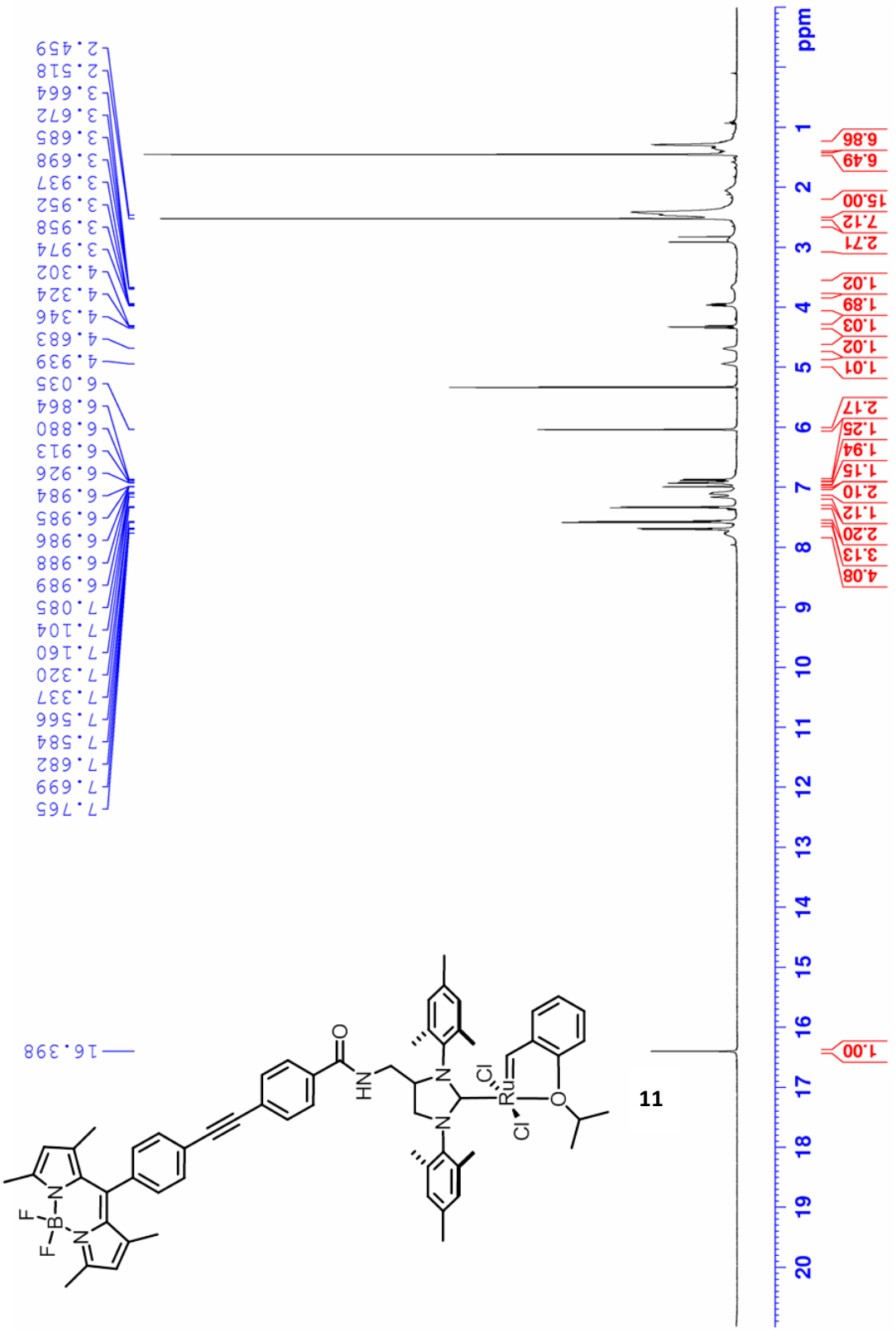

Figure S17. Amplification 1 of ^{1}H NMR spectrum of **11** (500 MHz, CD_2Cl_2).

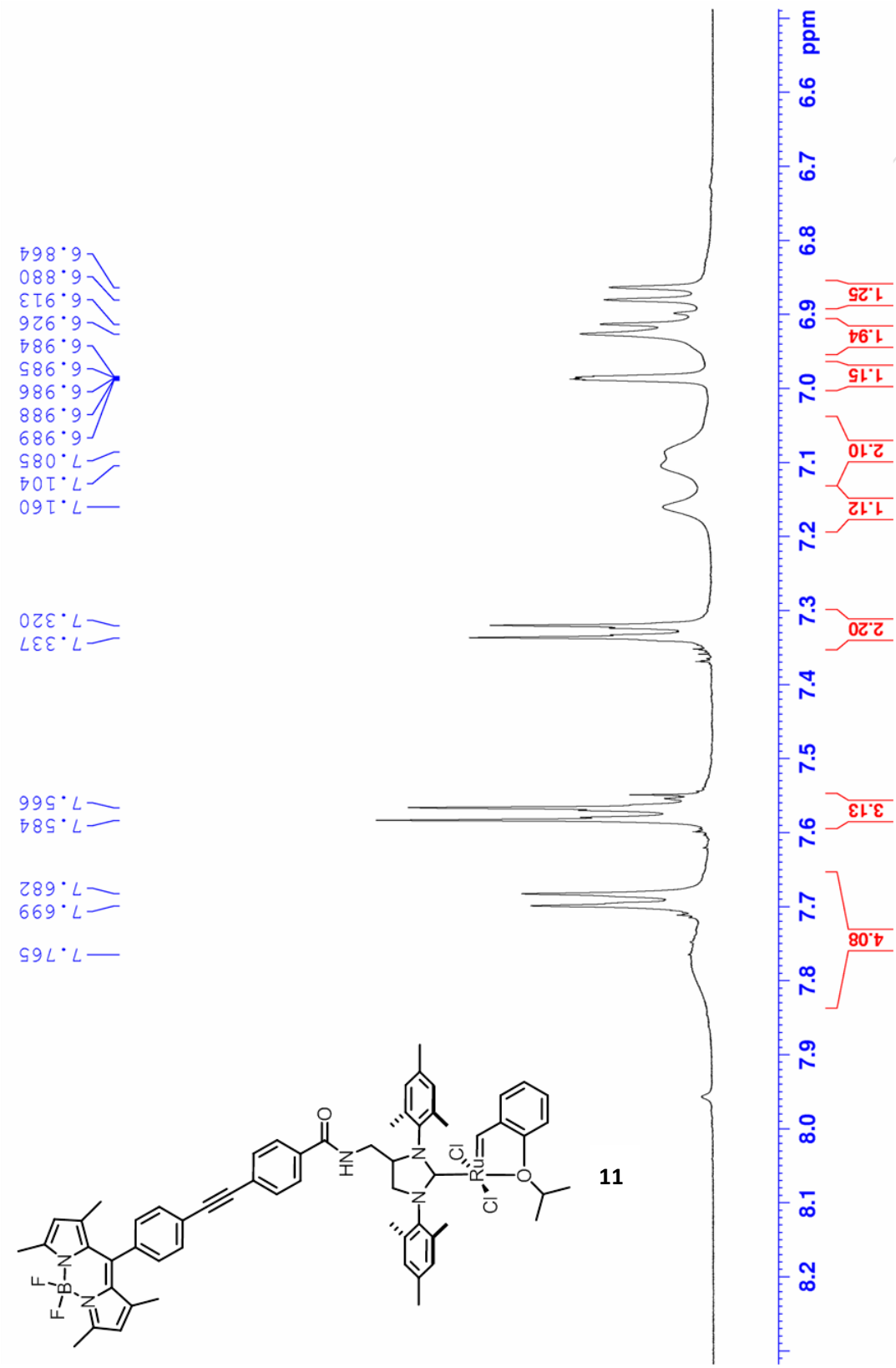

Figure S18. Amplification 2 of ^{1}H NMR spectrum of **11** (500 MHz, CD_2Cl_2).

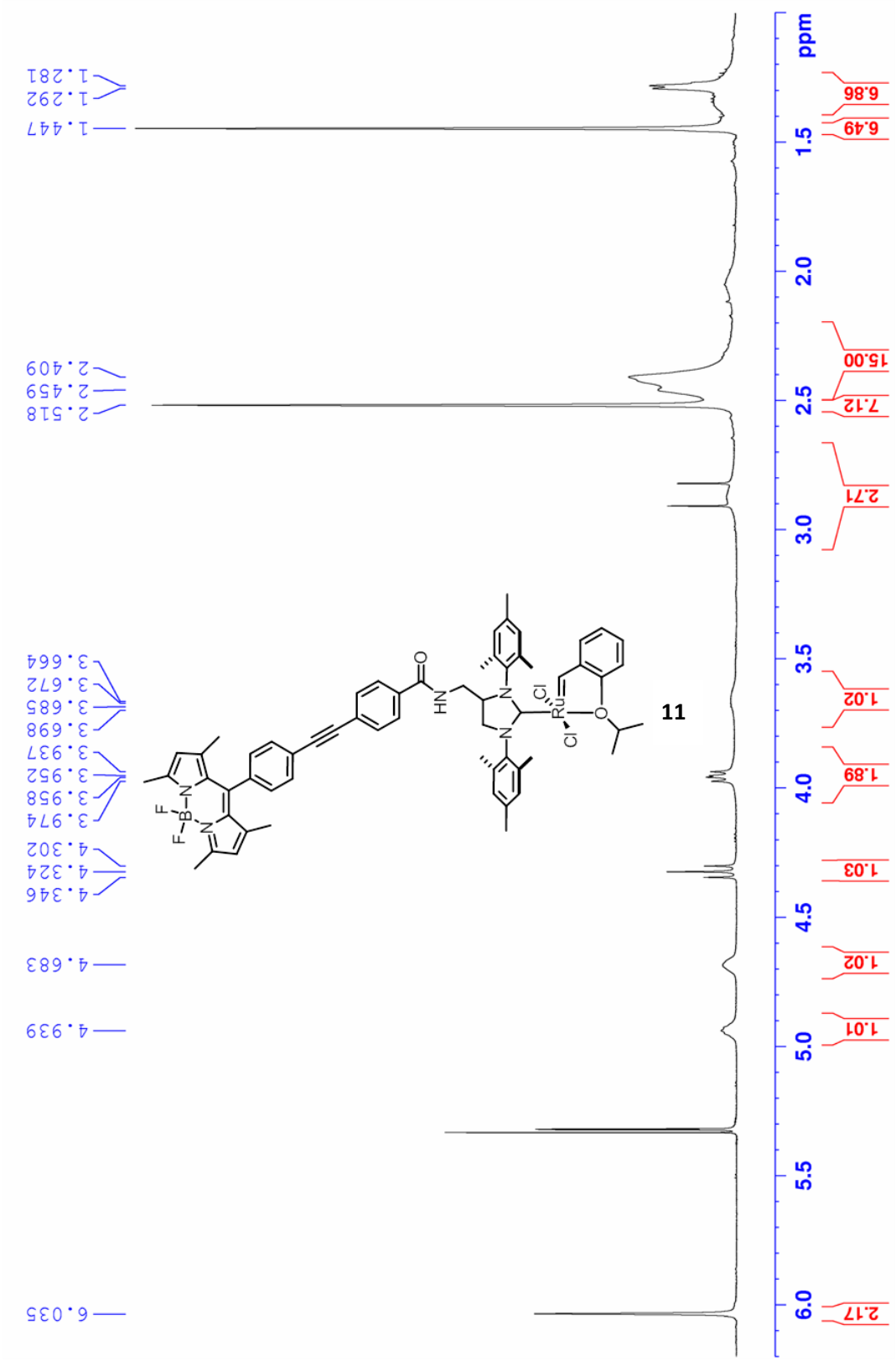

Figure S19. ^{13}C NMR spectrum of **11** (125 MHz, CD_2Cl_2).

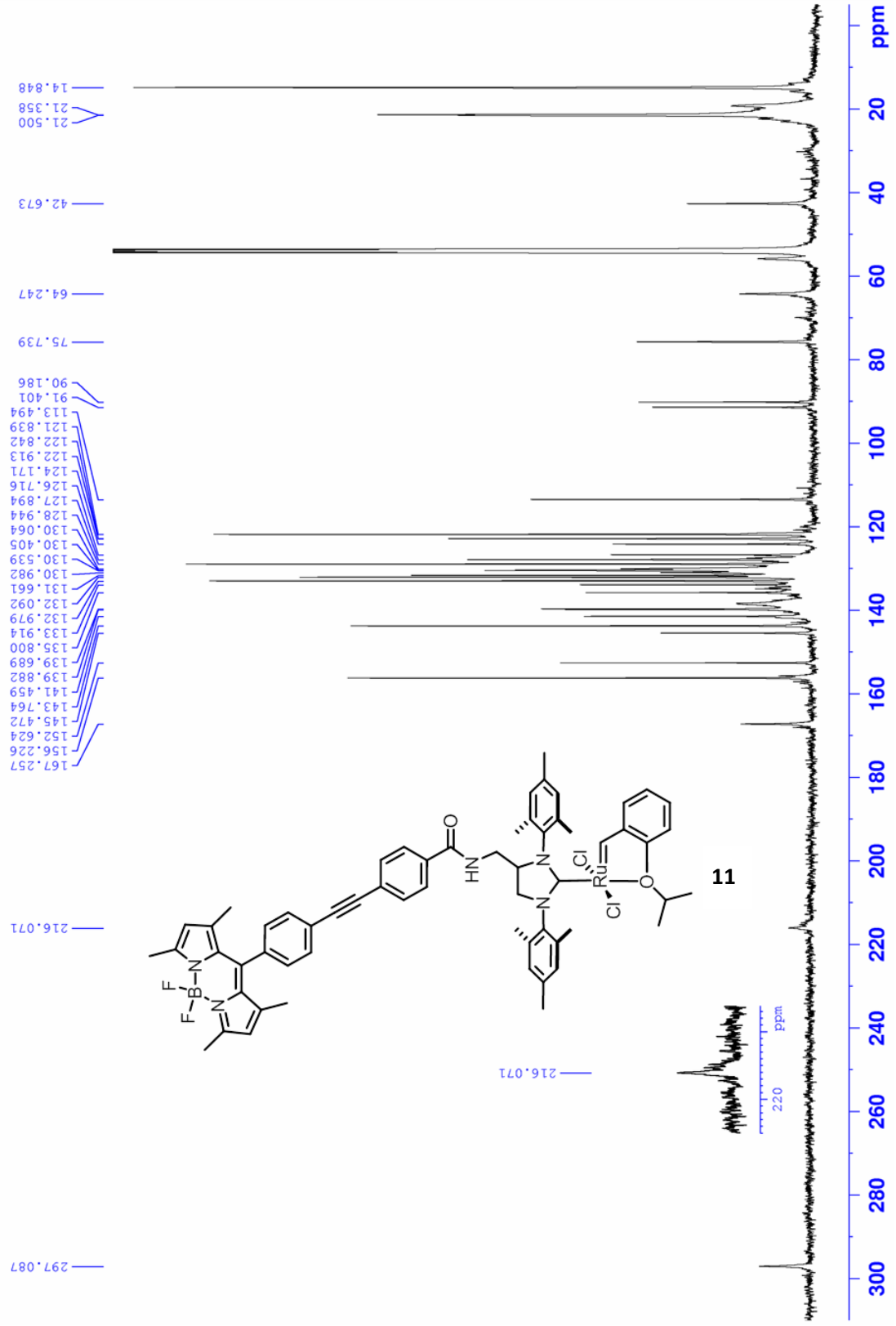

Figure S20. Amplification of ^{13}C NMR spectrum of **11** (125 MHz, CD_2Cl_2).